2009 spring

Advanced Physical Metallurgy

"Amorphous Materials"

06. 01. 2009

Eun Soo Park

Office: 33-316
Telephone: 880-7221
Email: espark@snu.ac.kr
Office hours: by an appointment

Glass-forming Ability Parameters

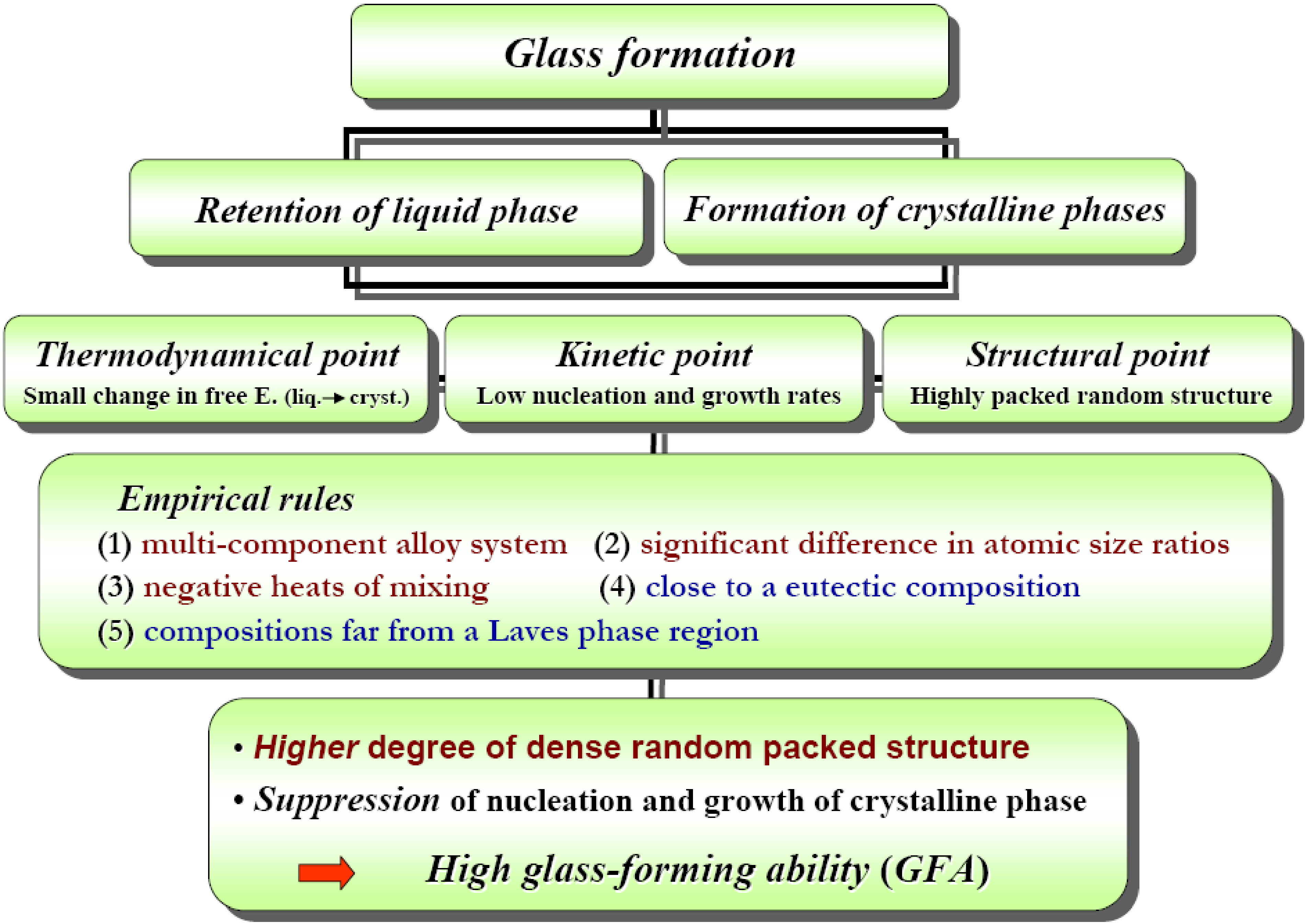
Glass formation
Retention of liquid phase
Formation of crystalline phases
Thermodynamical point
Small change in free E. (liq.→ cryst.)
Kinetic point
Low nucleation and growth rates
Structural point
Highly packed random structure
Empirical rules
(1) multi-component alloy system
(2) significant difference in atomic size ratios
(3) negative heats of mixing
(4) close to a eutectic composition
(5) compositions far from a Laves phase region
• Higher degree of dense random packed structure
• Suppression of nucleation and growth of crystalline phase
High glass-forming ability (GFA)

GFA Parameters on the basis of thermodynamic or kinetic aspects :

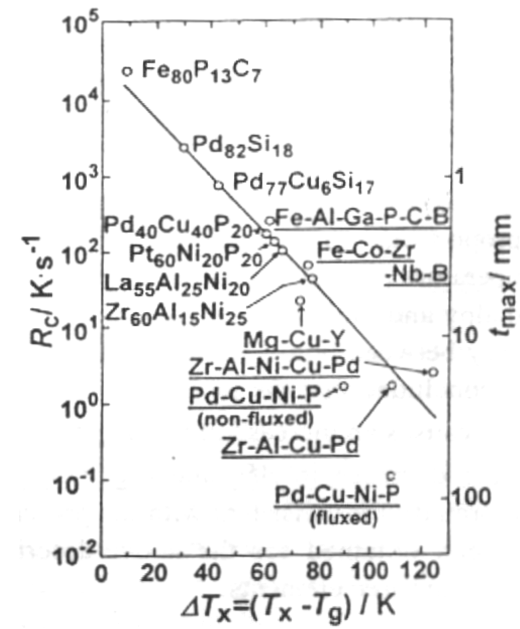

1) ΔT_x parameter = T_x - T_g

- quantitative measure of glass stability toward crystallization upon reheating the glass above T_g: stability of glass state
- cannot be considered as a direct measure for GFA

2) K parameter = $(T_x-T_g)/(T_l-T_x)$ = $\Delta T_x/(T_l-T_x)$

- based on thermal stability of glass on subsequent reheating
- includes the effect of T_l , but similar tendency to ΔT_x

3) ΔT^* parameter = $(T_m^{mix} - T_l)/\ T_m^{mix}$

- $T_m^{mix} = \sum_i^n n_i \cdot T_m^i$ (where n_i and T_m^i are the mole fraction and melting point, respectively, of the *i* th component of an *n*-component alloy.)

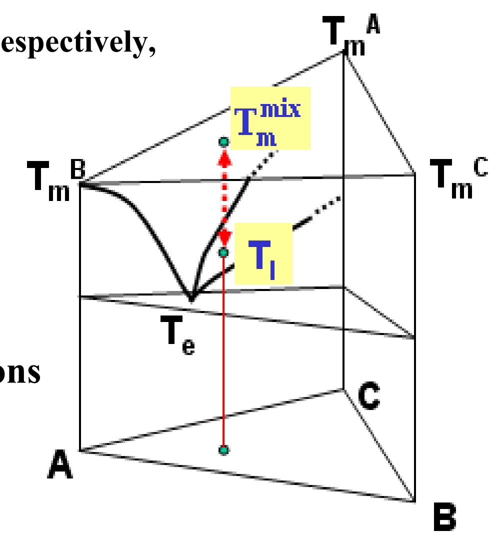

- evaluation of the stability of the liquid at equilibrium state
- alloy system with deep eutectic condition ~ good GFA
- for multi-component BMG systems: insufficient correlation with GFA

→ T_m^{mix} represents the fractional departure of T_m with variation of compositions and systems from the simple rule of mixtures melting temperature

GFA Parameters on the basis of thermodynamic or kinetic aspects :

4) T_{rg} parameter = T_g/T_l

- kinetic approach to avoid crystallization before glass formation
- Viscosity at T_g being constant, the higher the ratio T_g/T_l, the higher will be the viscosity at the nose of the CCT curves, and hence the smaller R_c
- T_l ↓ and T_g ↑ ► lower nucleation and growth rate ► GFA ↑

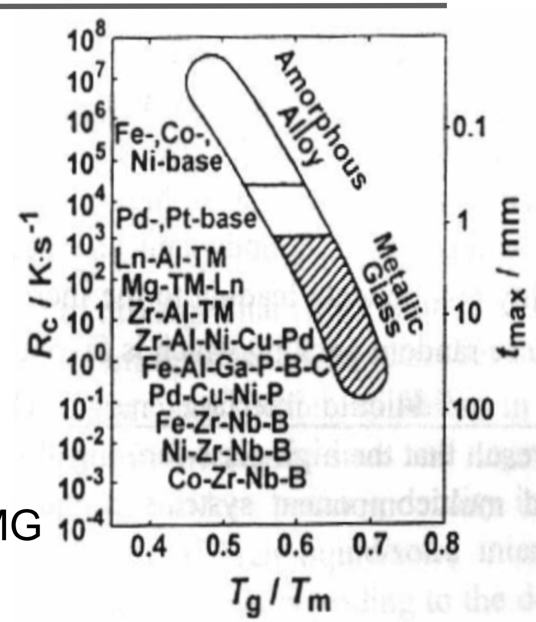

▪ significant difference between T_l and T_g in multi-component BMG

▪ insufficient information on temperature-viscosity relationship

► insufficient correlation with GFA

5) ɣ parameter = $T_x / (T_l + T_g)$

- thermodynamic and kinetic view points - **relatively reliable parameter**
- stability of equilibrium and metastable liquids: T_l and T_g
- resistance to crystallization: T_x

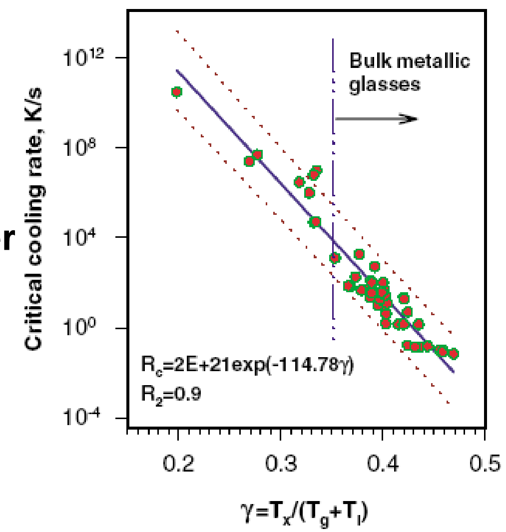

No universal model **to predict and evaluate what families of alloy compositions are likely to form BMGs**

Combination of categories

that are viewed as decisive in the formation of amorphous alloys

New criterion

for predicting and evaluating Glass Forming Ability

- **useful guideline for BMG alloy system design**

- save time and experimental cost

→ **new alloy system with enhanced GFA**

Approach 1. combine thermodynamic and structural points

$$\sigma = \Delta T^* \times \quad P'$$

ΔT^* : **Relative decrease of melting temp.** $\boldsymbol{P'}$: **Effective atomic mismatch per solute atom**

$$\Delta T^* = \frac{T_m^{mix} - T_l}{T_m^{mix}}$$

$$P' = \frac{C_B}{C_B + C_C}\left|\frac{v_B - v_A}{v_A}\right| + \frac{C_C}{C_B + C_C}\left|\frac{v_C - v_A}{v_A}\right|$$

(where, $T_m^{mix} = \sum x_i T_m^i$, x_i = molefraction, T_m^i = melting point)

(where, C_i(i=A,B,C) = solute content, ν_i = atomic volume)

Approach 2. combine thermodynamic and kinetic points

$$\varepsilon \;=\; \frac{\Delta T_m + \Delta T_x + T_x}{T_m^{mix}}$$

$\Delta Tm + \Delta Tx$: ***Liquid phase stability*** + $\boldsymbol{Tx}$: ***Resistance to cristallization***

(where, ΔTm = Tmmix – Tl , ΔTx = Tx – Tg)

(where, Tx = crystallization onset temperature)

σ parameter (thermodynamic and atomic configuration aspects)

ΔT^* : Relative decrease of melting temp.

→ liquid phase stability

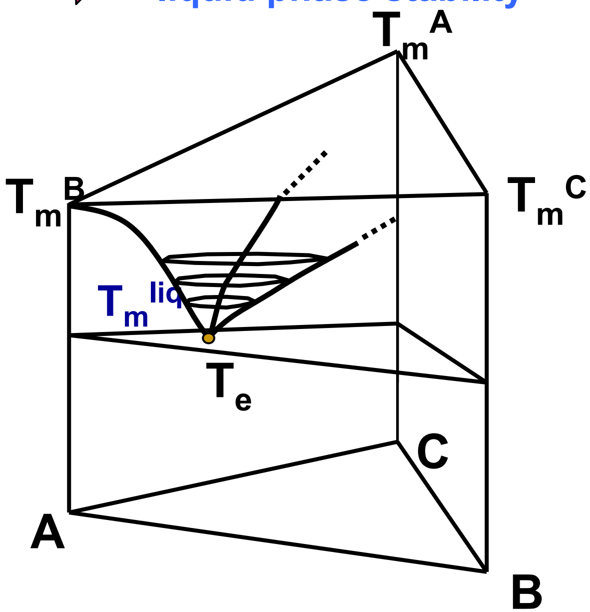

Deep eutectic condition

P' : Effective atomic mismatch per solute atom

→ solid phase stability

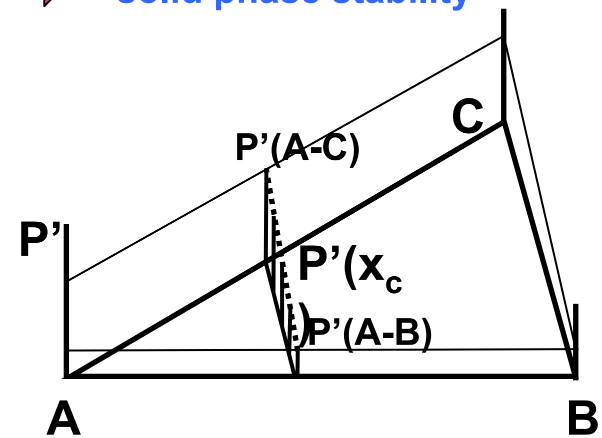

$$P'_{(A-B)} \leq P'(Xc) \leq P'_{(A-C)}$$

Large difference in atomic size

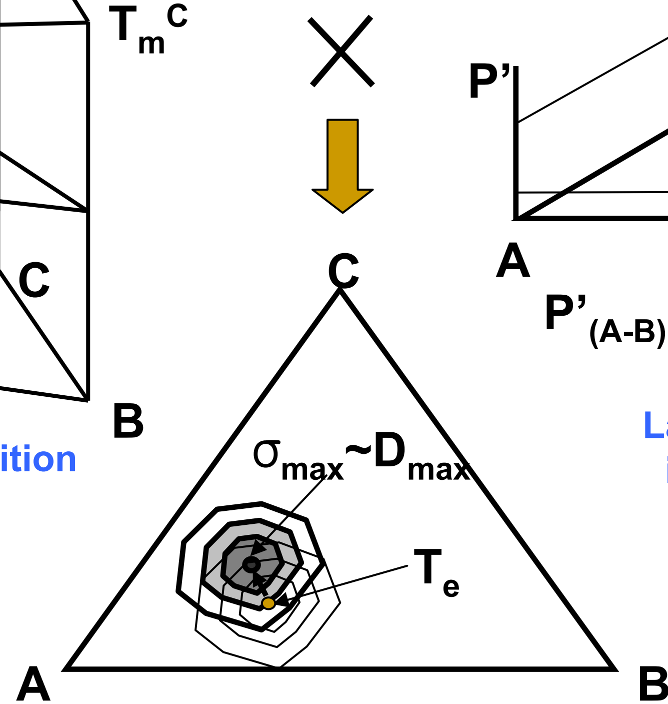

New criterion for GFA, σ parameter $\sigma = \Delta T^* \times P'$

* Appl. Phys. Lett., 86, 061907 (2005)

ε parameter (thermodynamic and kinetic aspects)

*** CCT curve showing temperature range for ε parameter***

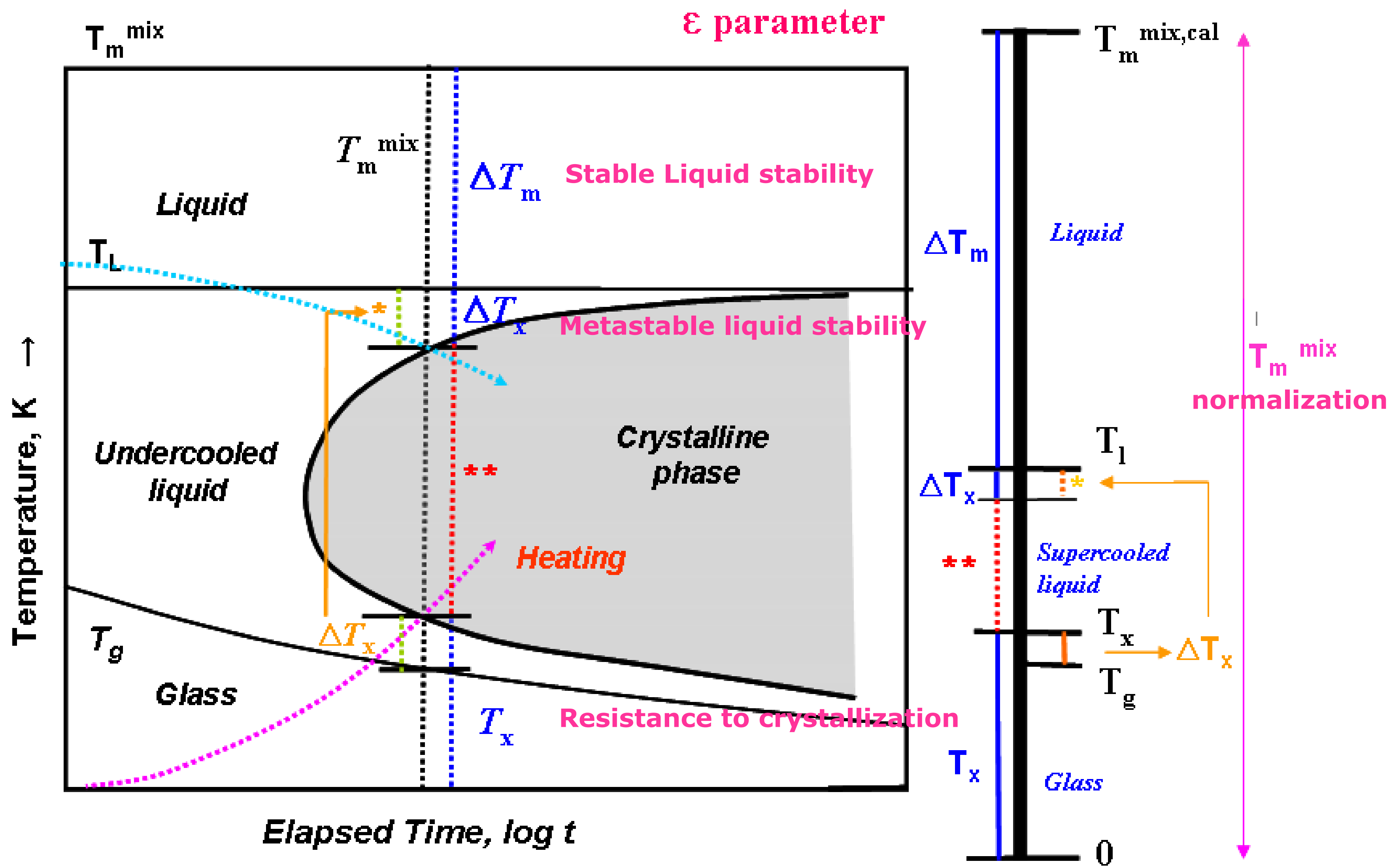

Recent BMGs with critical size ≥ 10 mm

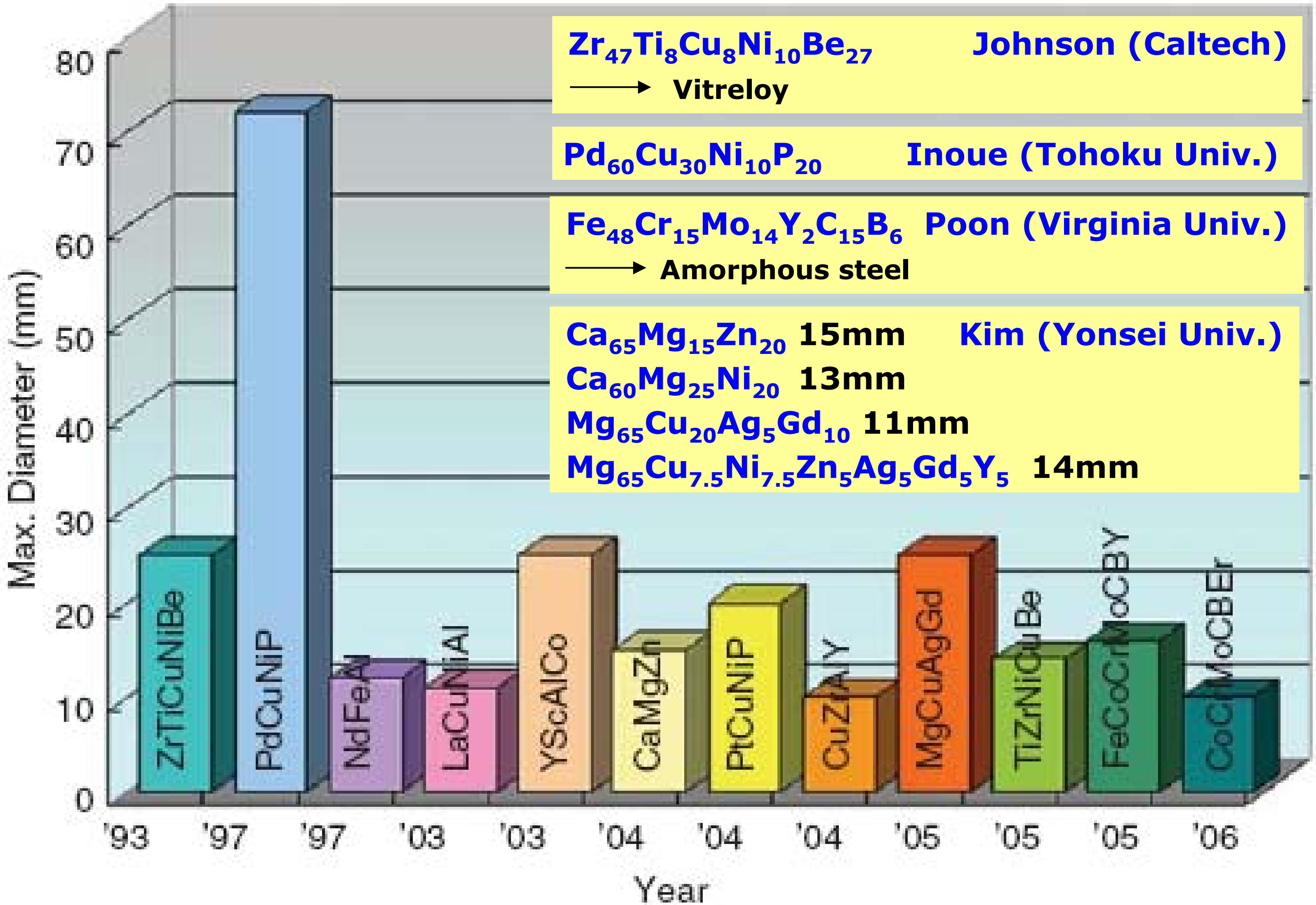

A.L. Greer, E. Ma, MRS Bulletin, 2007; 32: 612.

Bulk glass formation in the $Pd_{40}Ni_{10}Cu_{30}P_{20}$ system

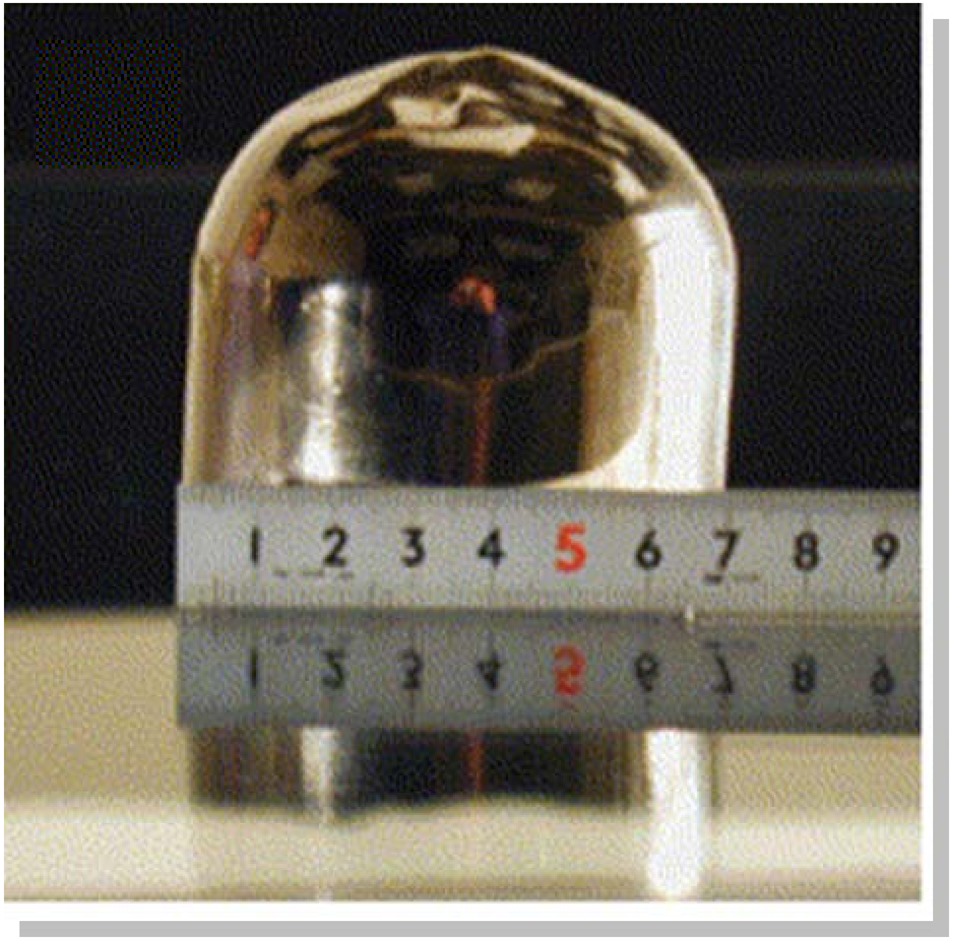

- **Largest ingot**

maximum diameter for glass formation : 72 mm

Critical cooling rate: ~ 0.1K/sec.

High strength of Bulk Metallic Glasses

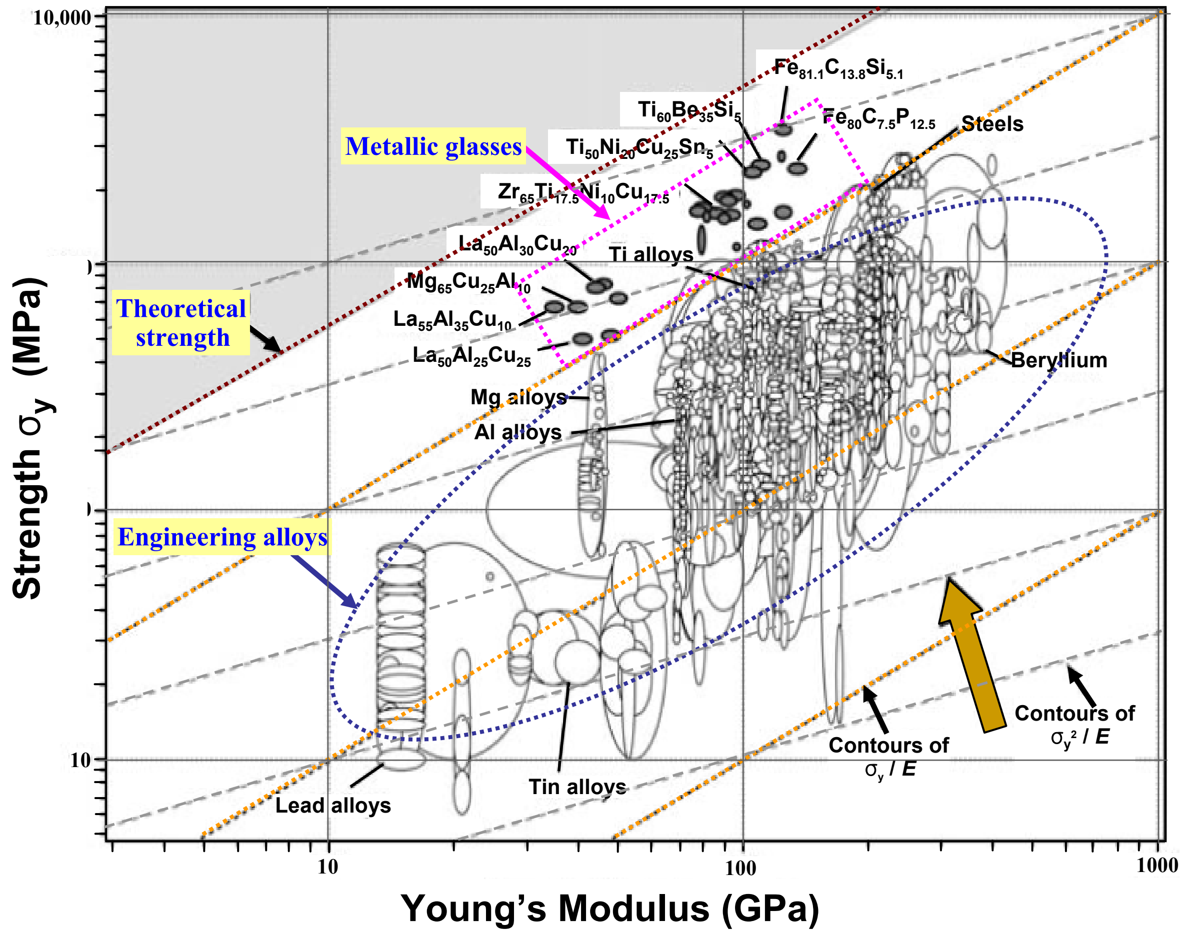

High fracture strength over 5 GPa in Fe-based BMGs

A.L. Greer, E. Ma, MRS Bulletin, 2007; 32: 612.

Limited Plasticity by shear softening and shear band

- **Microscopically brittle fracture**

  ➡ **Death of a material for structural applications**

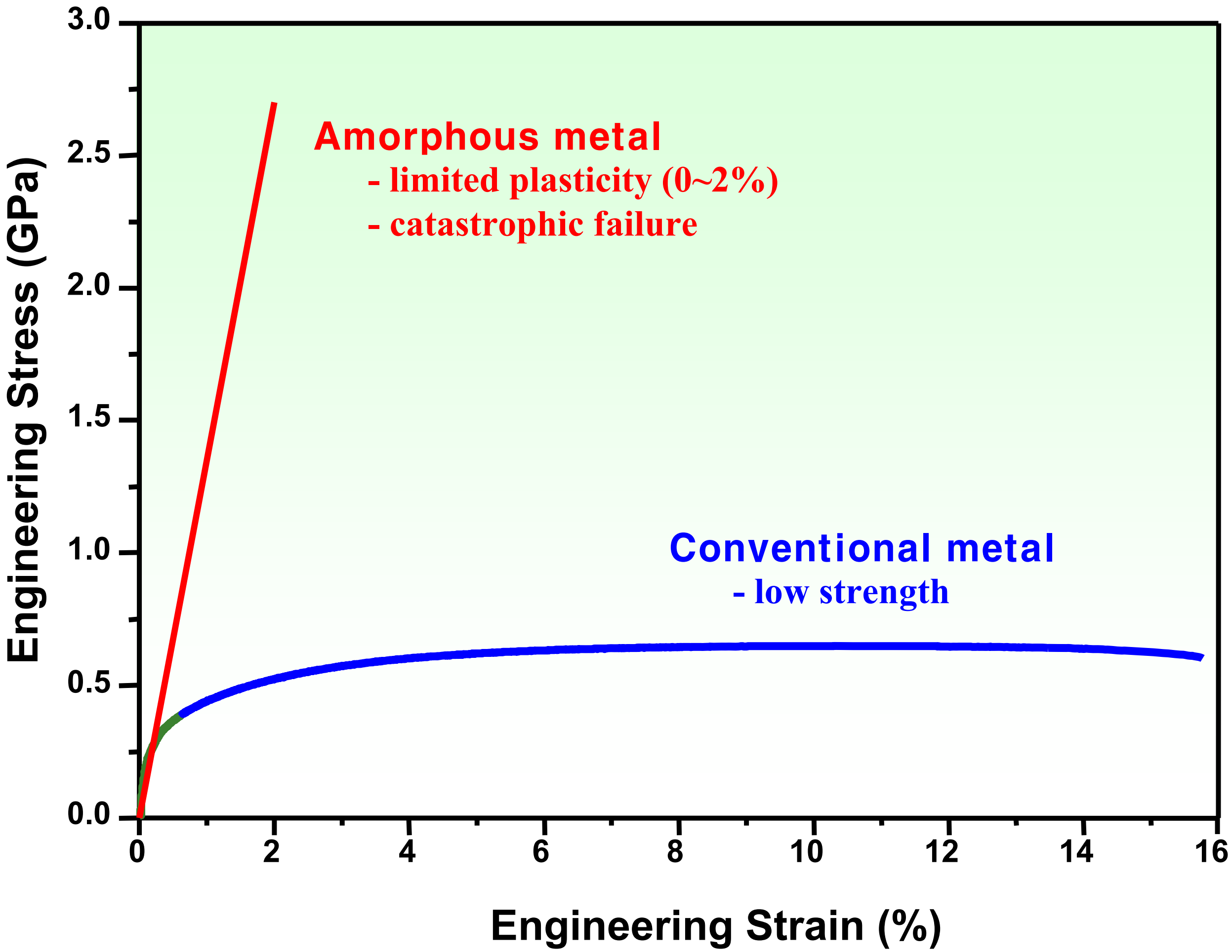

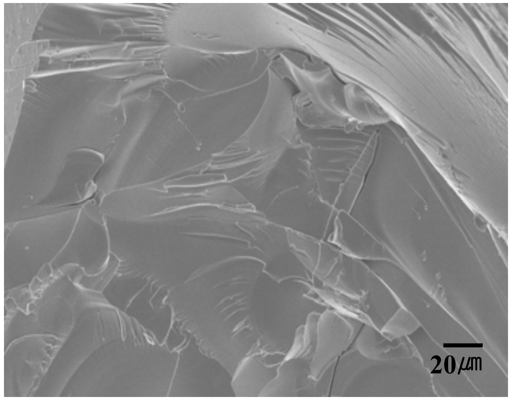

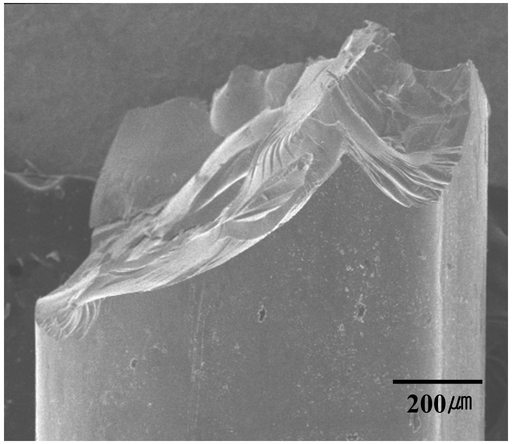

What governs plasticity in metallic glasses?

Plastic deformation in metallic glasses

Plastic deformation in metallic glass

- *No* dislocation / *No* slip plane
- Inhomogeneously localized plastic flow in the shear band

interrupt the localization of stress and deformation

- Prevent propagation of single shear band ⇨ BMG matrix composites
- Multiple shear band formation

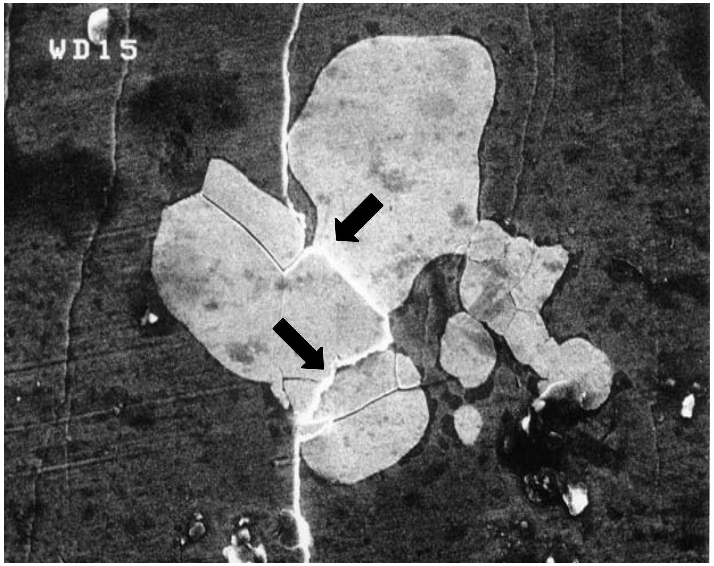

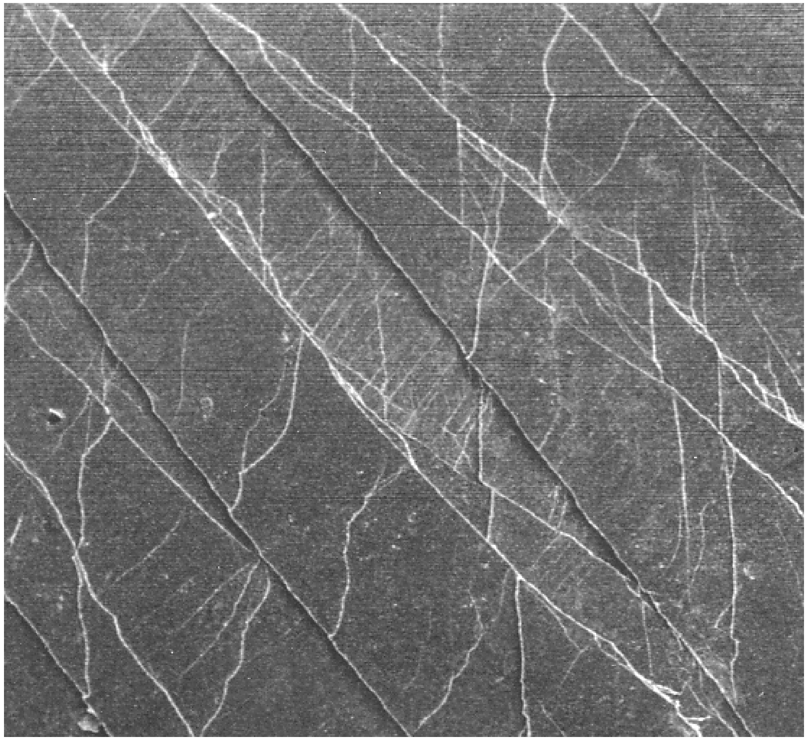

Ex-situ BMG matrix composites

1) Casting : hard/ductile particle

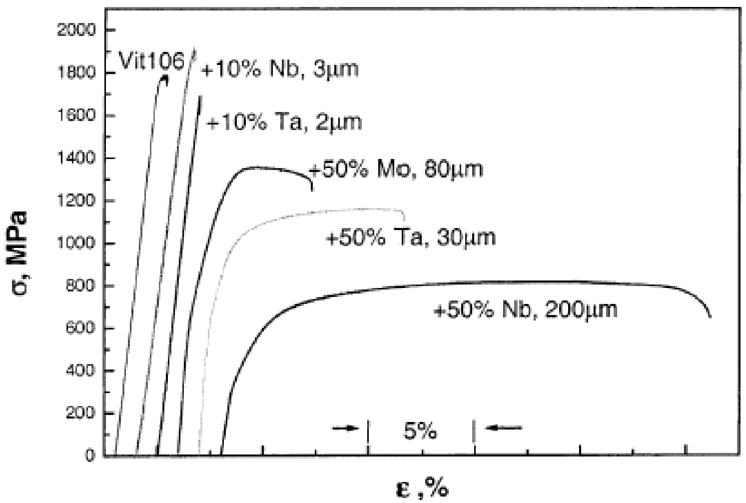

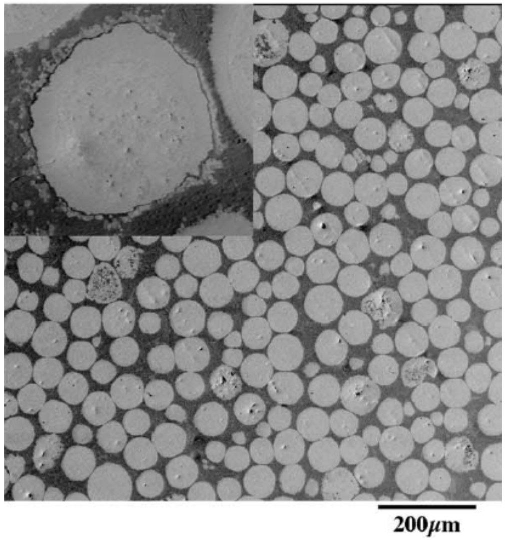

(Johnson et al., Acta Mater.,1999)

2) Extrusion : ductile powder

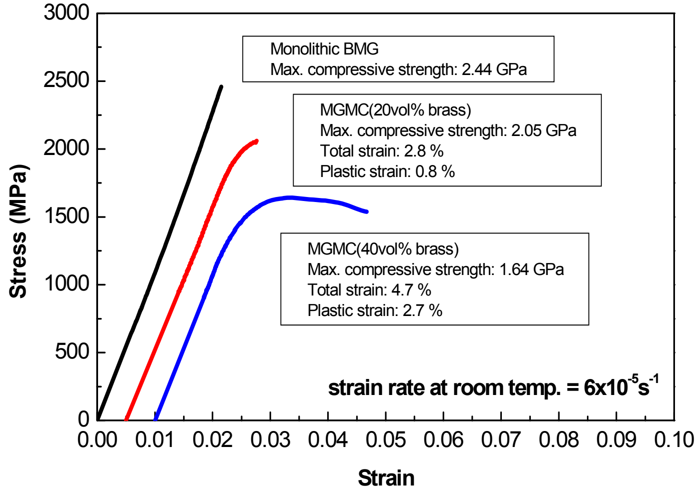

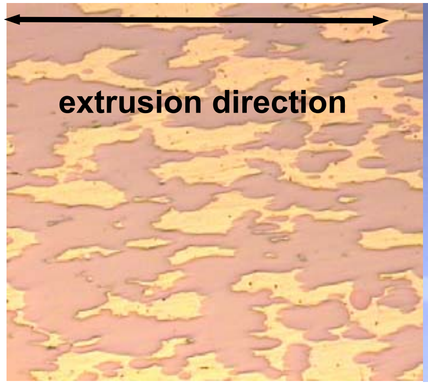

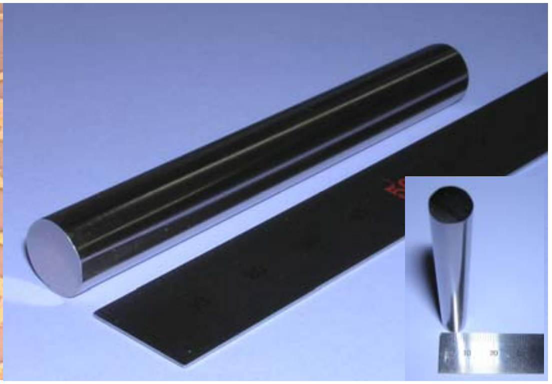

(Kim et al., J. Non-cryst. Solids, 2002)

In-situ BMG matrix composites

1) Solidification : formation of primary ductile phase

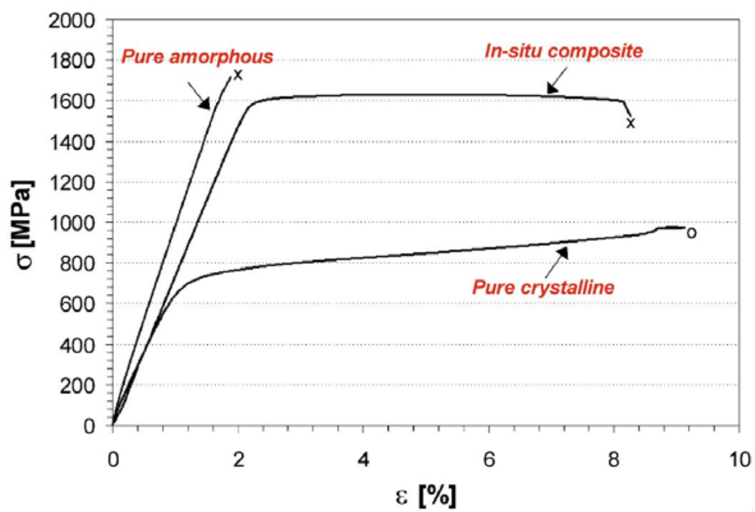

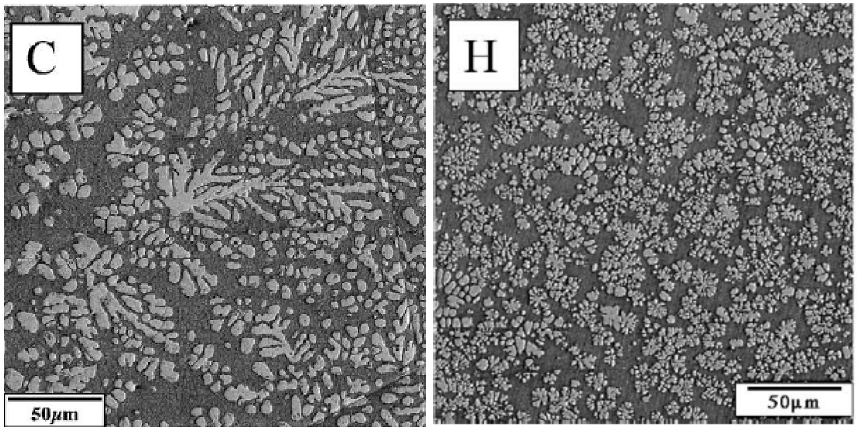

(Johnson et al., Acta Mater., 2001)

2) Solidification : precipitation of ductile phase

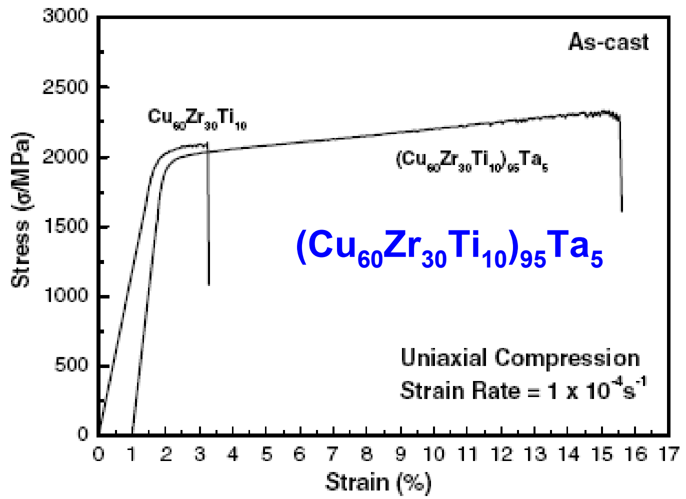

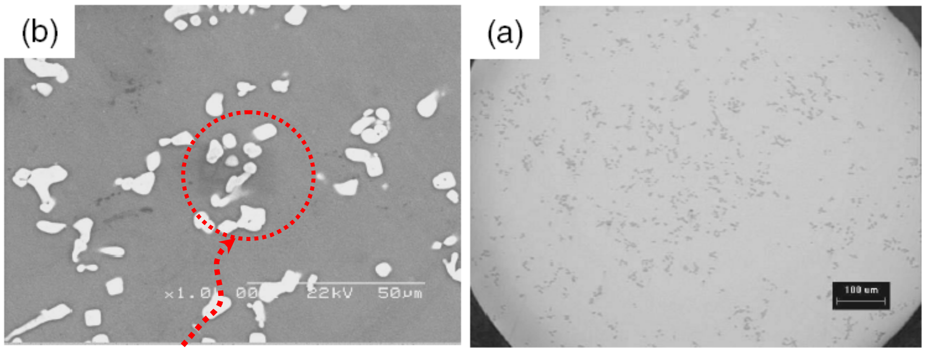

Ta rich particle

(Johnson et al., Acta Mater., 2001)

Size of heterogeneity

Shear bands are ~20 nm in width

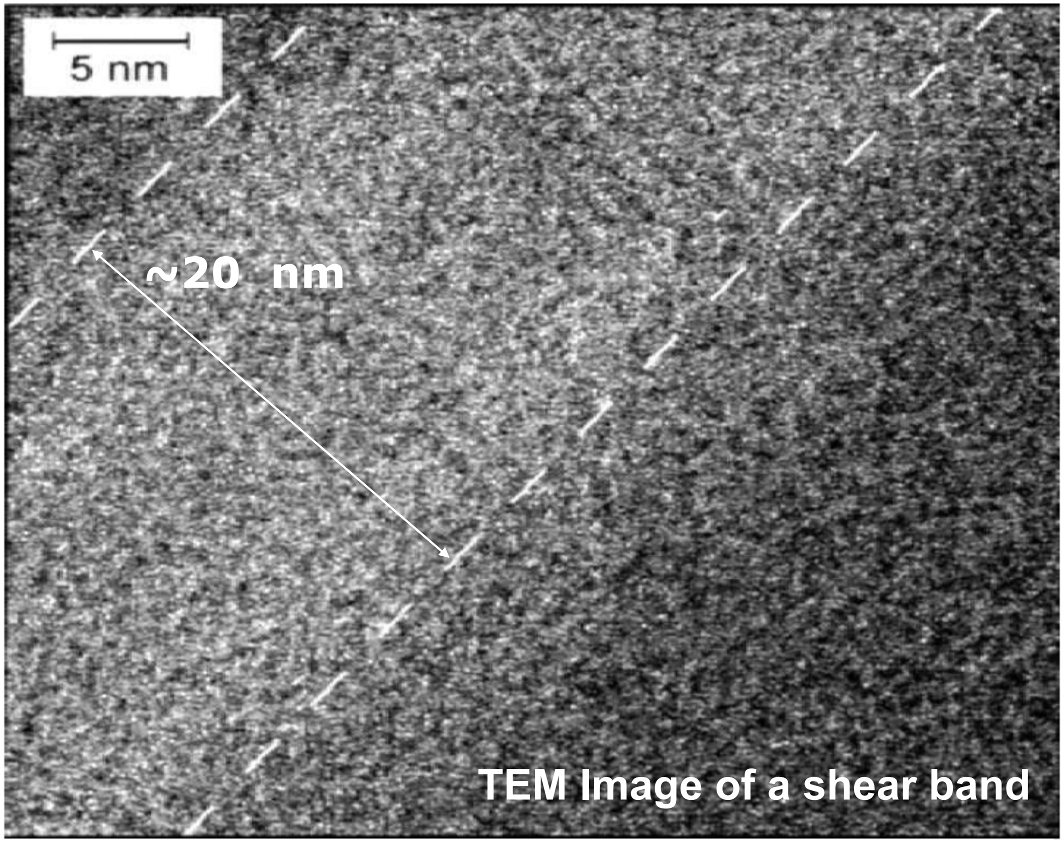

- **Prevent propagation of single shear band**

➡ **Micro- or nanometer scale heterogeneity**

Size of heterogeneity

- Elementary flow event in an metallic glasses

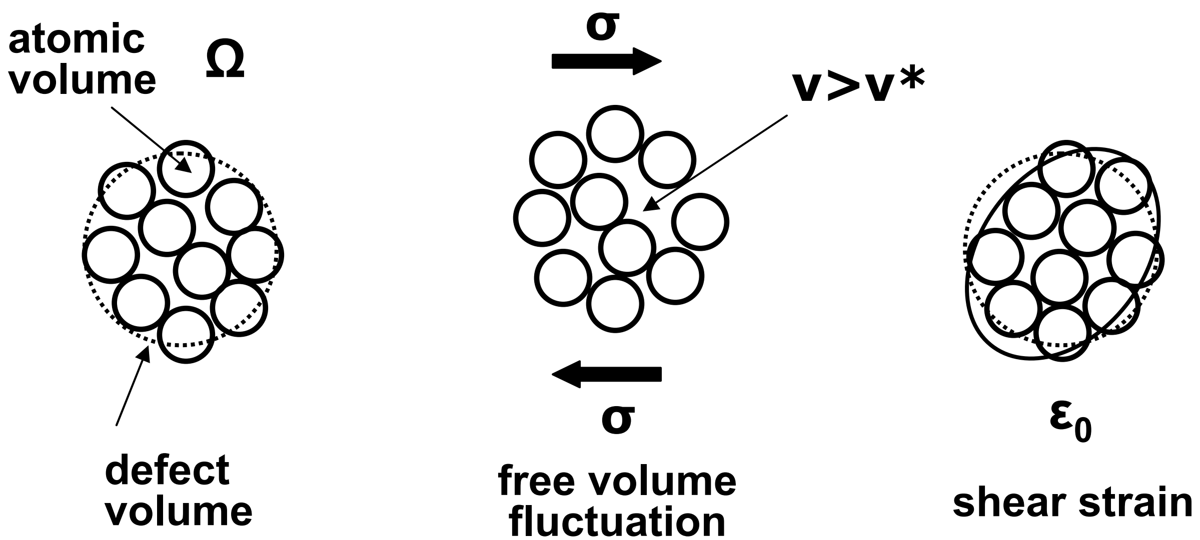

Probability $\exp(A\frac{v^*}{v_f})$

average free volume

Flow governed by localized defect (~10 atoms) and creates defects

atomic scale heterogeneity

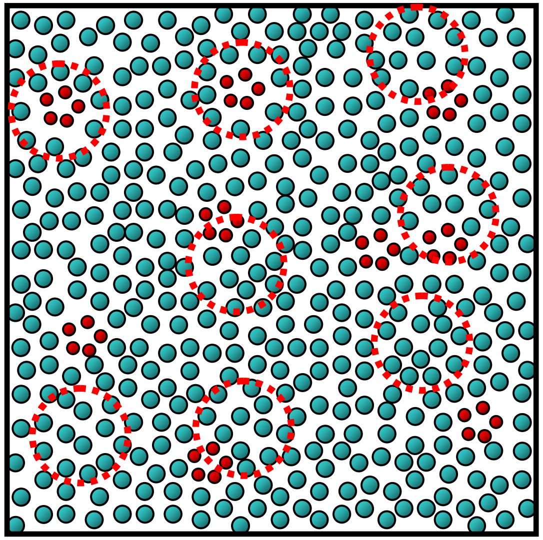

$$\eta = \eta_0 \exp\left\{A\frac{V_0}{V_f}\right\}$$

Plastic deformation in metallic glasses

- Flow governed by localized defect (~10 atoms)

- Flow creates defects

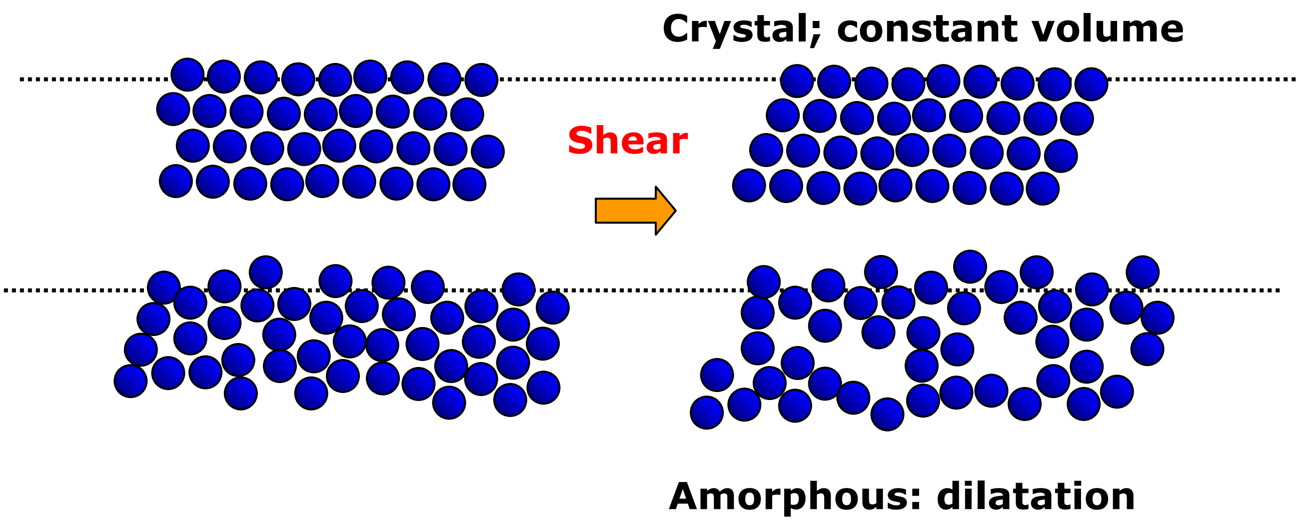

- Shear bands form by accumulation of defects

Understanding how shear bands form and propagate in metallic glasses

Fragility

- Fragility ~ extensively use to figure out liquid dynamics and glass properties corresponding to "frozen" liquid state

< Classification of glass >

Strong network glass **: Arrhenius behavior**

$$\eta = \eta_0 \exp[\frac{E_a}{RT}]$$

Fragile network glass **: Vogel-Fulcher relation**

$$\eta = \eta_0 \exp[\frac{B}{T - T_0}]$$

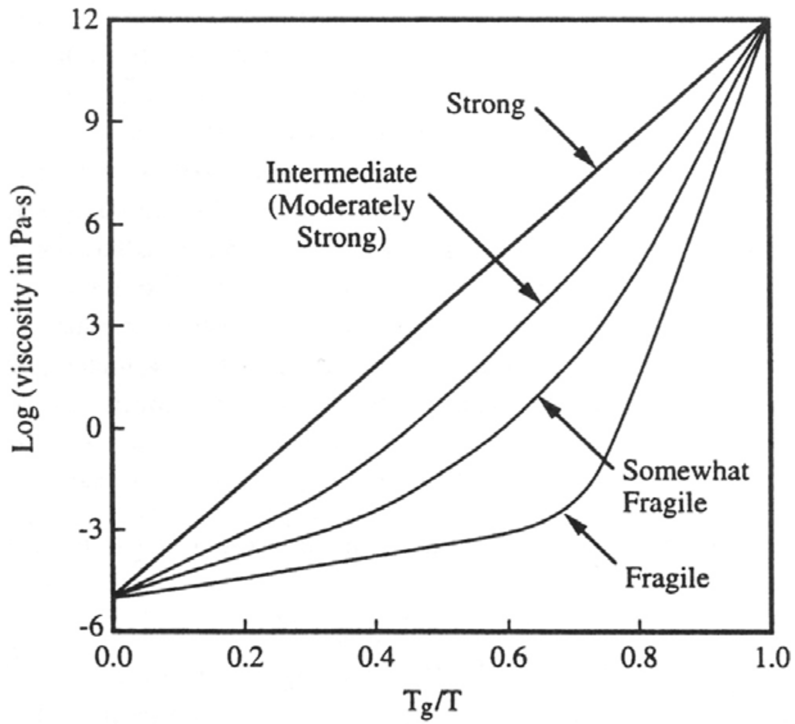

< Quantification of Fragility >

$$m = \left.\frac{d \log \eta(T)}{d(T_{g,n}/T)}\right|_{T=T_{g,n}} = \left.\frac{d \log \tau(T)}{d(T_g/T)}\right|_{T=T_g}$$

Slope of the logarithm of viscosity, η (or structural relaxation time, τ) at T_g

Correlation between fragility and plasticity

- **Correlation between elastic constants and plasticity**

Low G/B → ***High ν*** → **shear collapse**

(shear modulus / bulk modulus) ***(poisson's ratio)*** ***(multiple shear band)***

Jan Schroers et al, , Phys. Rev. Lett. 93, 255506 (2004).

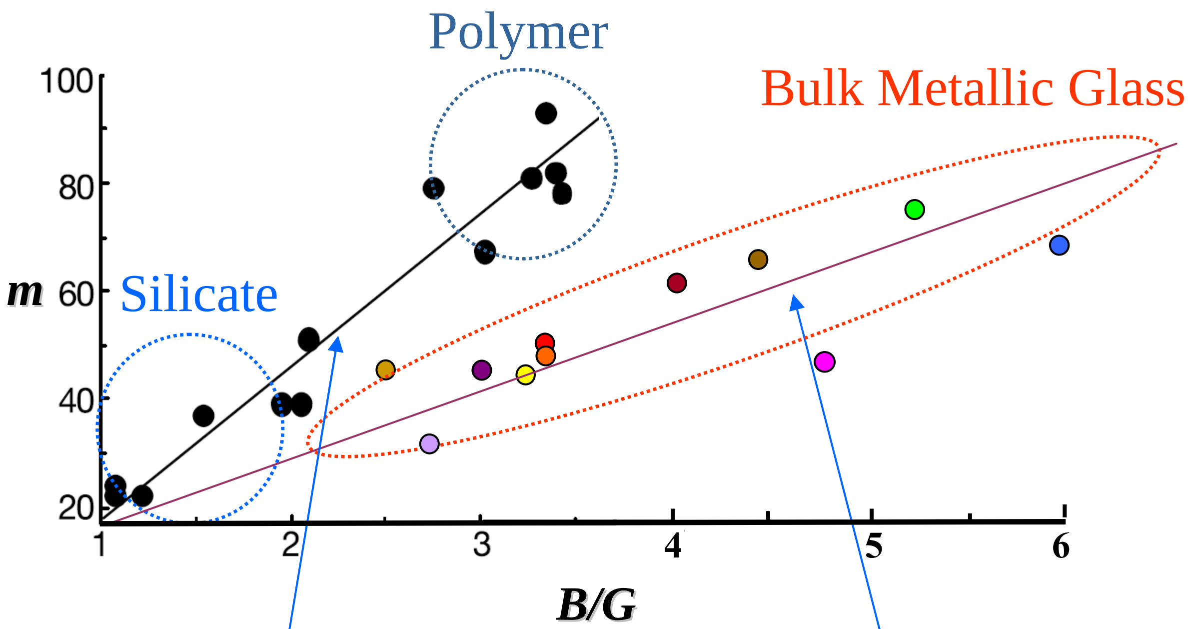

$$m-17=29(B/G-1)$$

$$m-17=14(B/G-1)$$

*** J. Mater. Res. 23, 523 (2008)**

Correlation between fragility and plasticity

Low G/B
High ν ➡ *High m*
(*fragility index*) ➡ Large Plasticity
(*multiple shear band*)

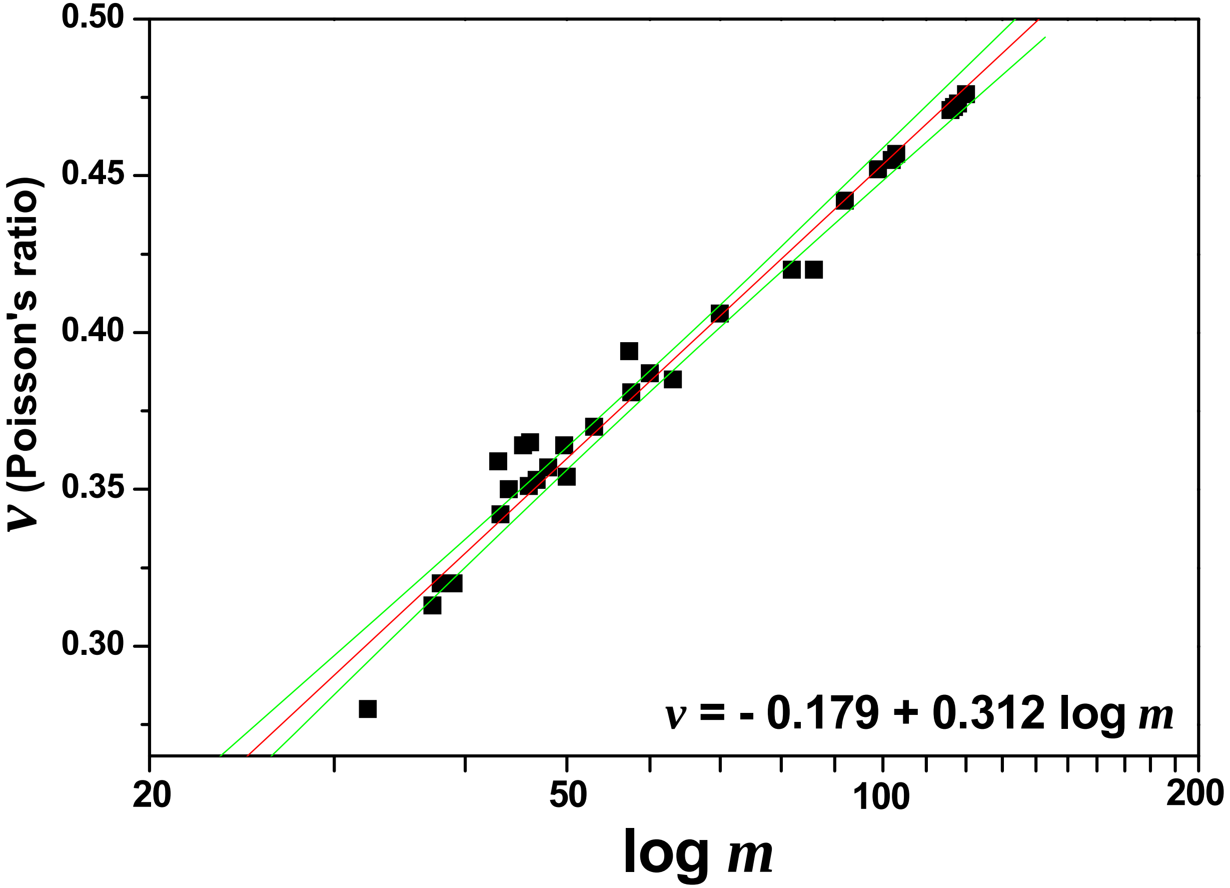

* Appl. Phys. Lett., 91, 031907.

Enhancement plasticity in BMGs with atomic scale heterogeneity

a) Effect of quenched-in quasicrystal nuclei

Effect of secondary phase in amorphous matrix

3 mm rod

(a) $Zr_{63}Ti_5Nb_2Cu_{15.8}Ni_{6.3}Al_{7.9}$

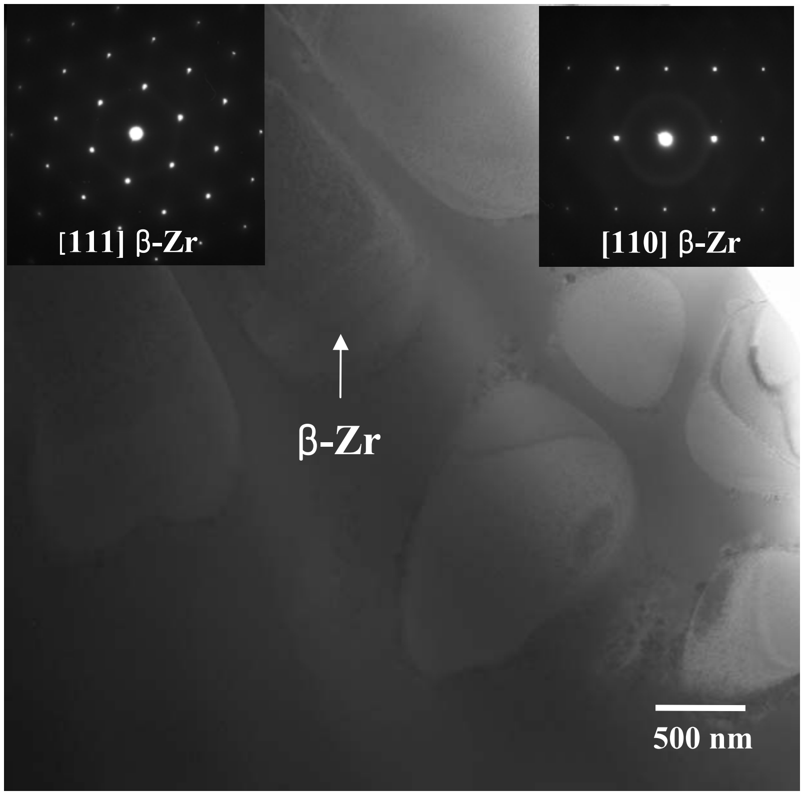

β-Zr dendrite in amorphous matrix

(b) $Zr_{57}Ti_8Nb_{2.5}Cu_{13.9}Ni_{11.1}Al_{7.5}$

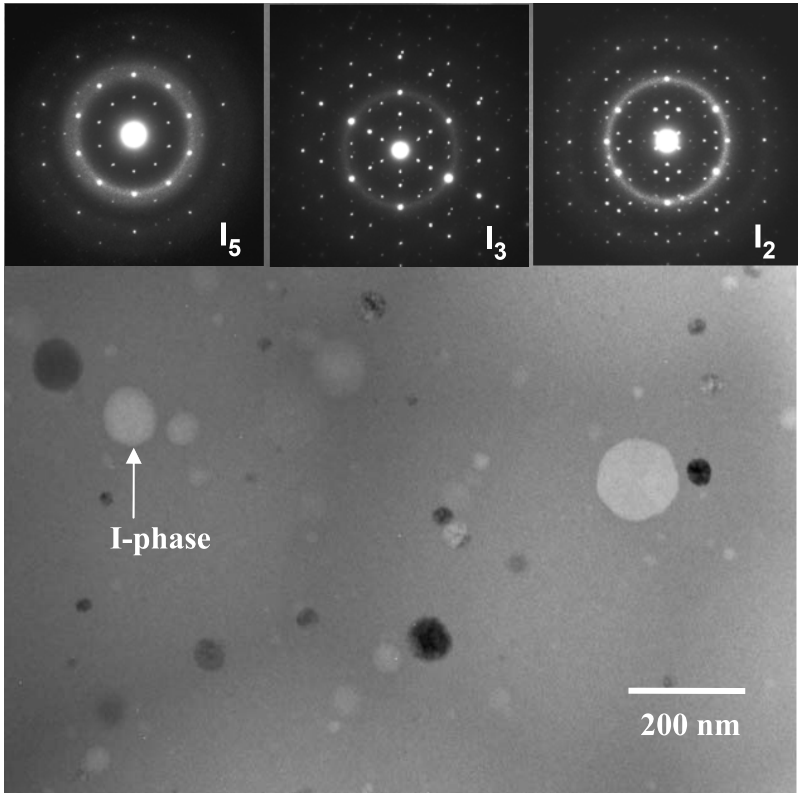

I-phase particle in amorphous matrix

Effect of secondary phase in amorphous matrix

* unpublished (2008)

- Compression test

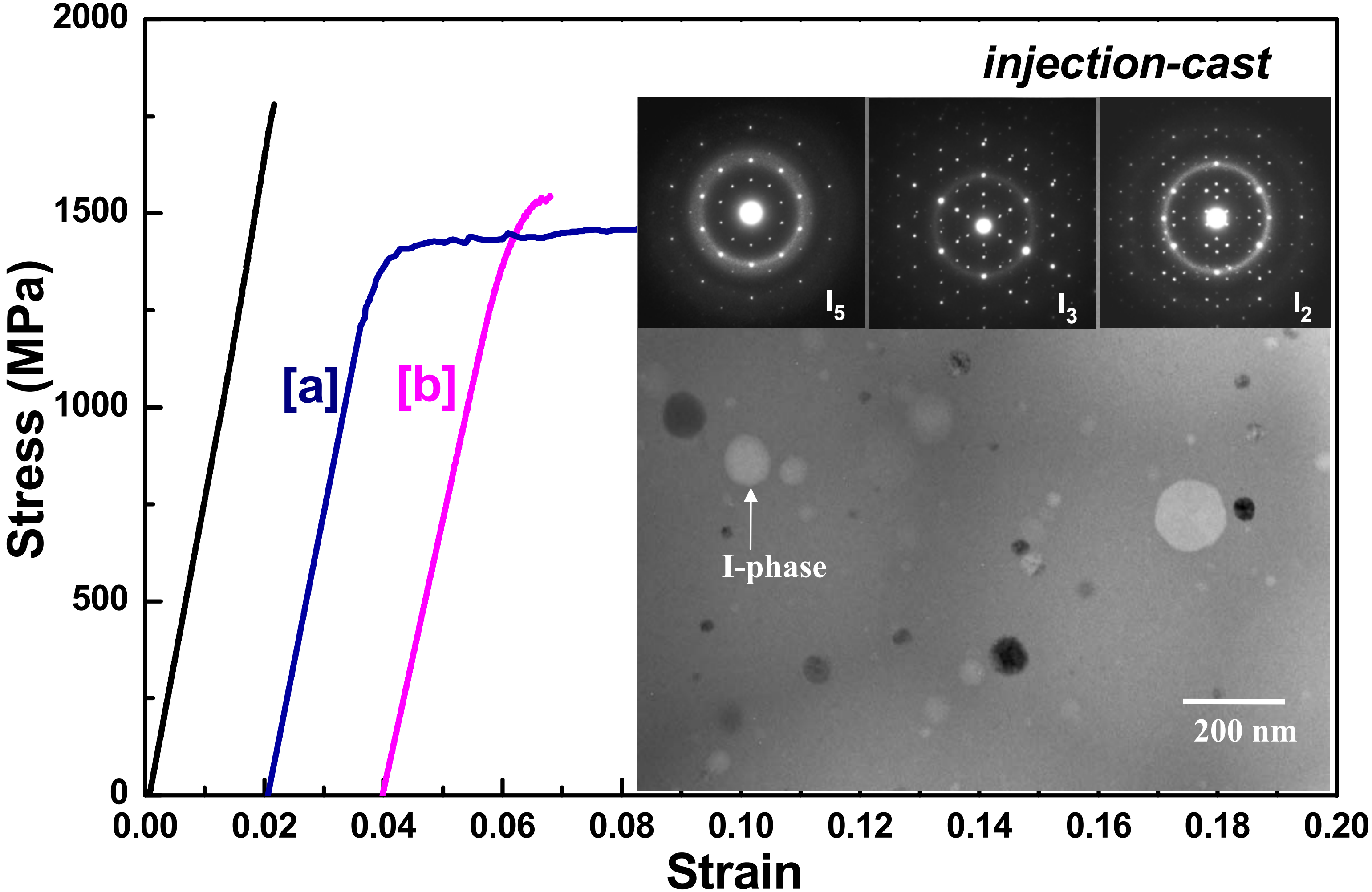

Continuous interface between amorphous and I-phase

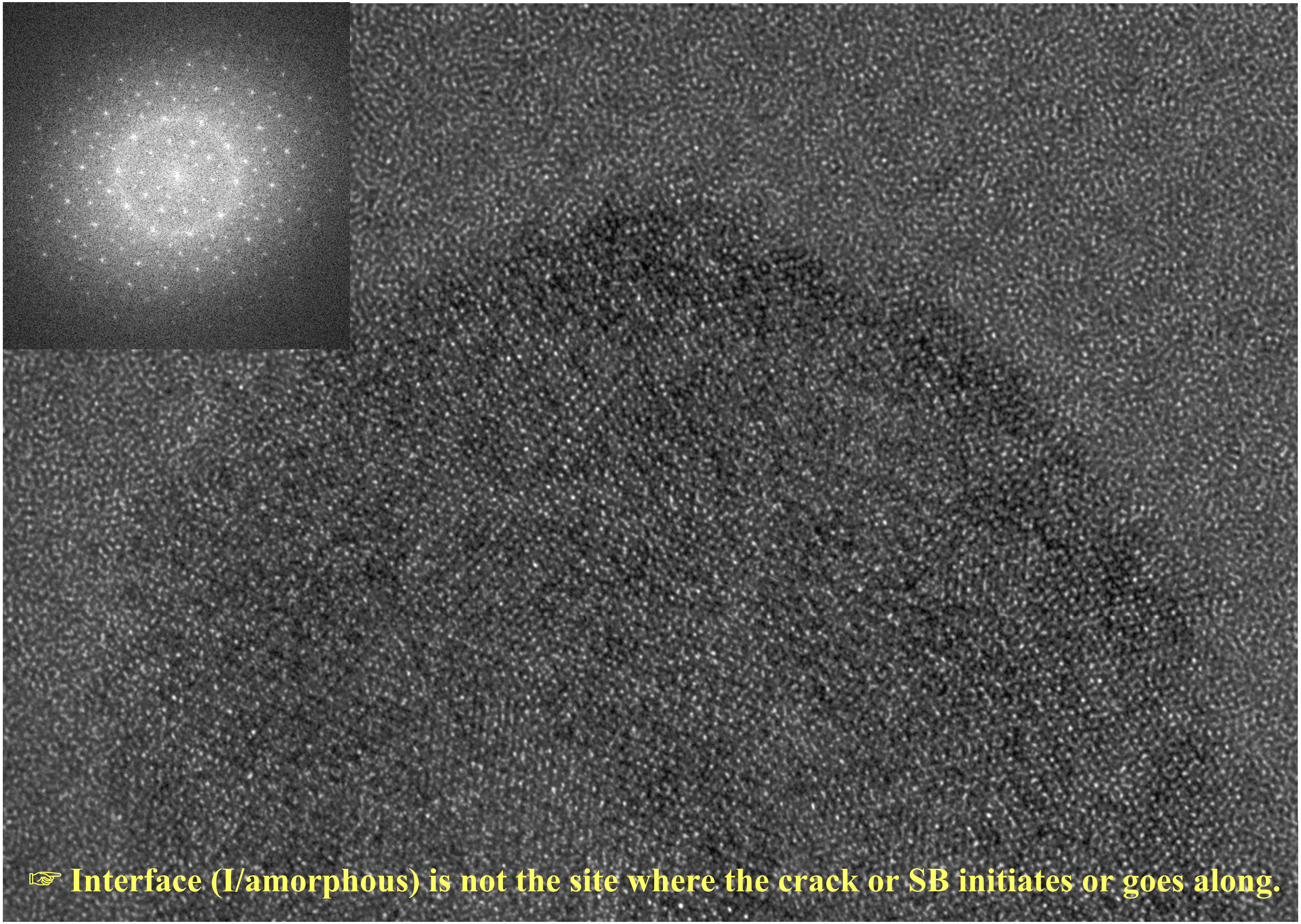

Role of icosahedral particle on the propagation of shear band

Before deformation

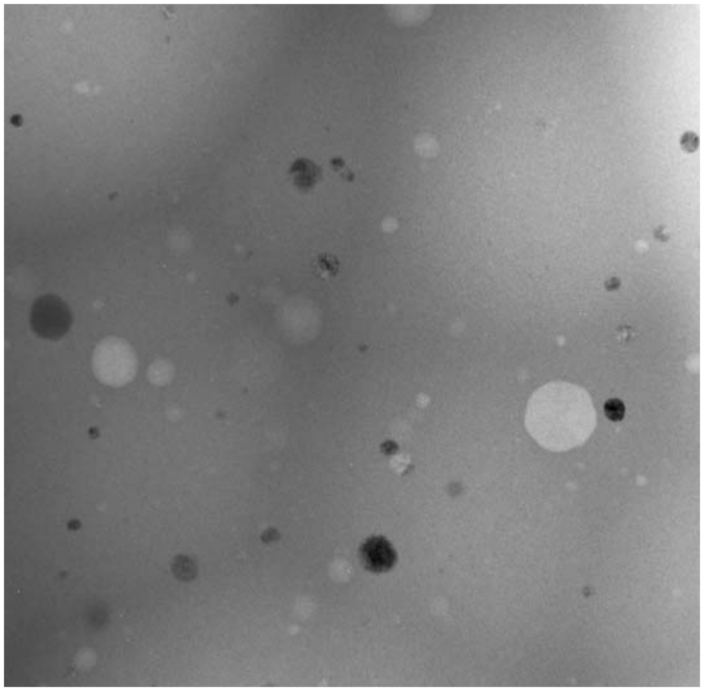

After deformation

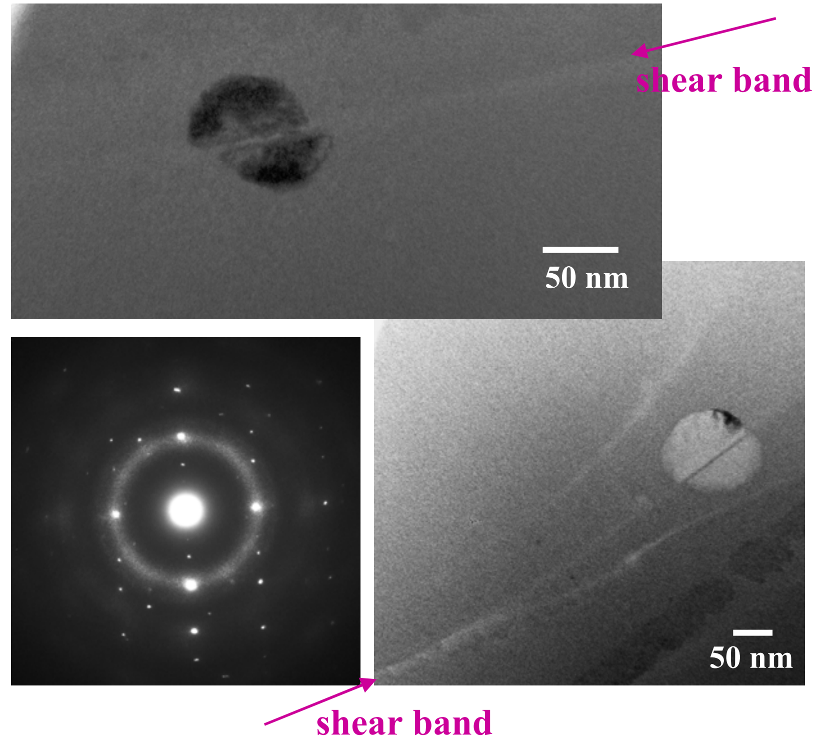

- **Shear band passes through icosahedral particle.**
- **Icosahedral particle splits across with the plastic deformation of metallic glass matrix**

☞ **No distribution of icosahedral particle to blocking the propagation of shear band.**

☞ **No enhancement of plasticity in MGMC with icosahedral particle**

Effect of quenched-in quasicrystal nuclei

2 mm rod

(a) $Zr_{63}Ti_5Nb_2Cu_{15.8}Ni_{6.3}Al_{7.9}$

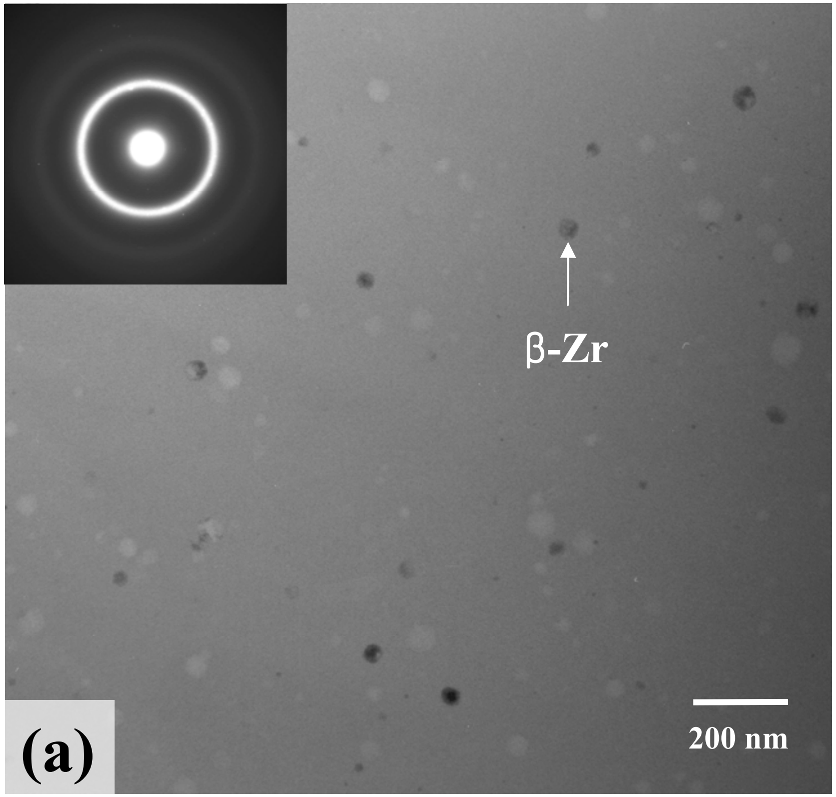

β-Zr particle(~70 nm) in amorphous matrix

(b) $Zr_{57}Ti_8Nb_{2.5}Cu_{13.9}Ni_{11.1}Al_{7.5}$

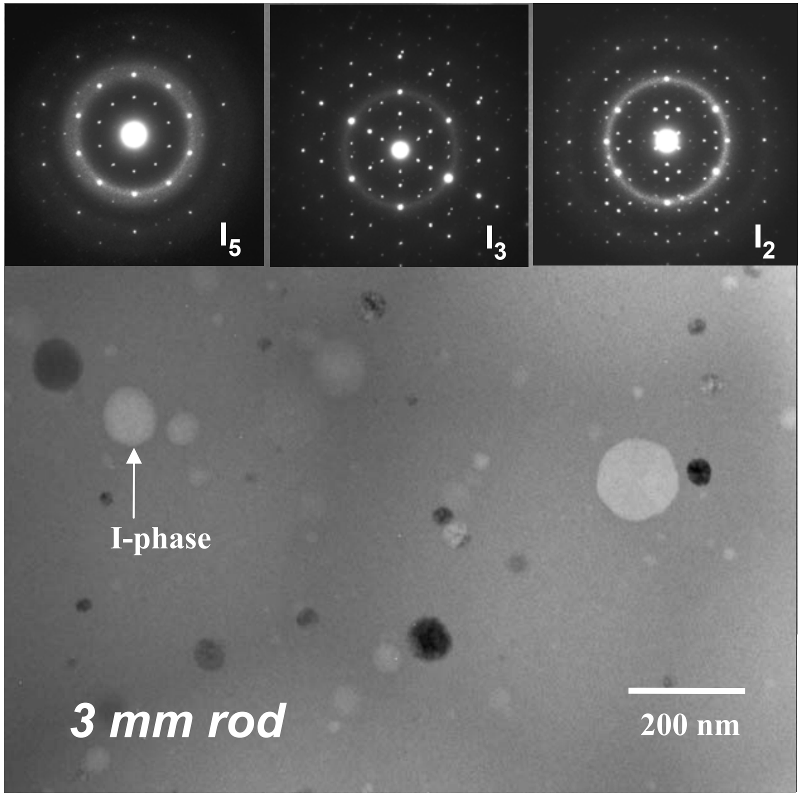

Fully amorphous structure

Effect of quenched-in quasicrystal nuclei

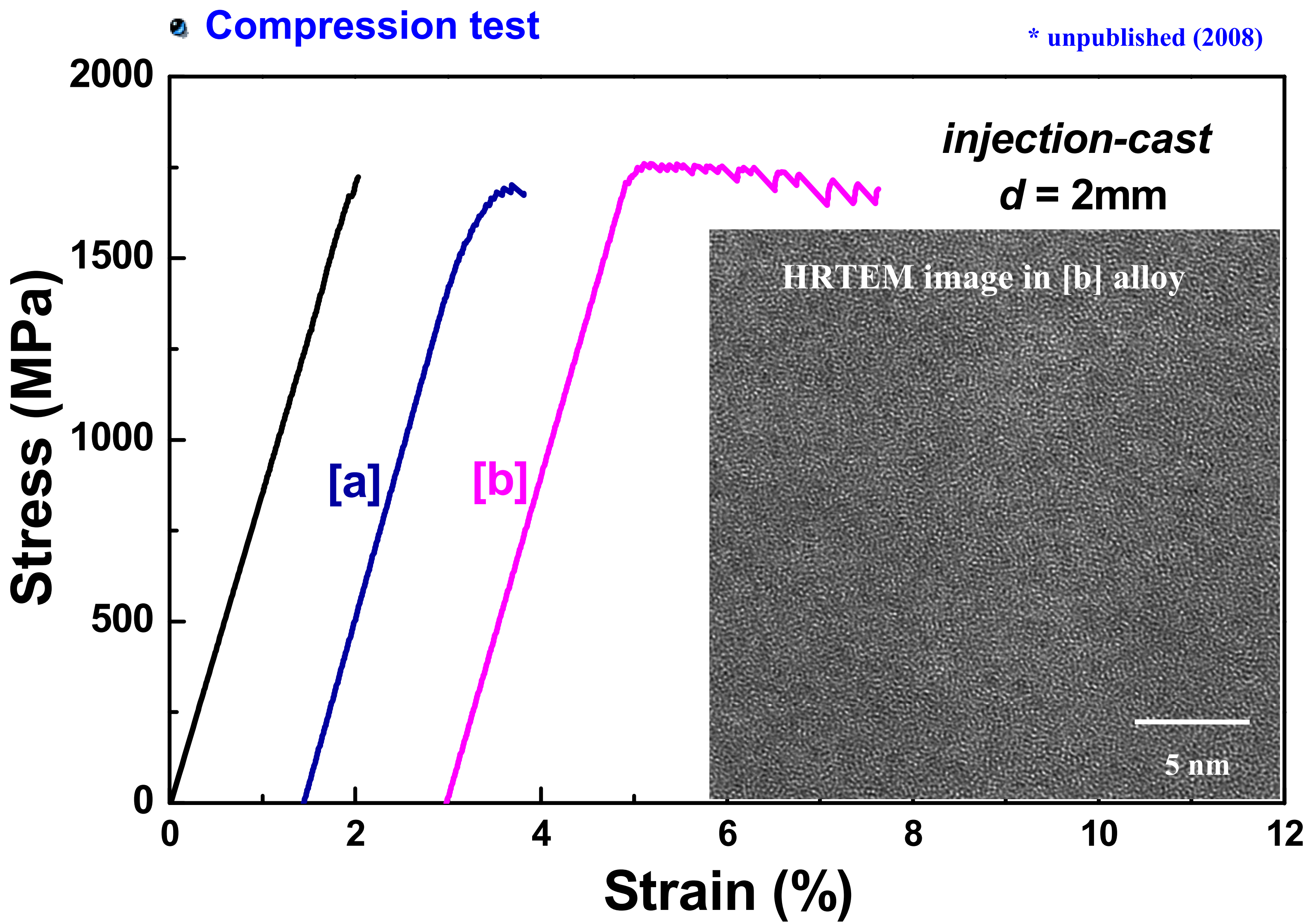

Effect of quenched-in quasicrystal nuclei

- *Activation E : driving force for nucleation*

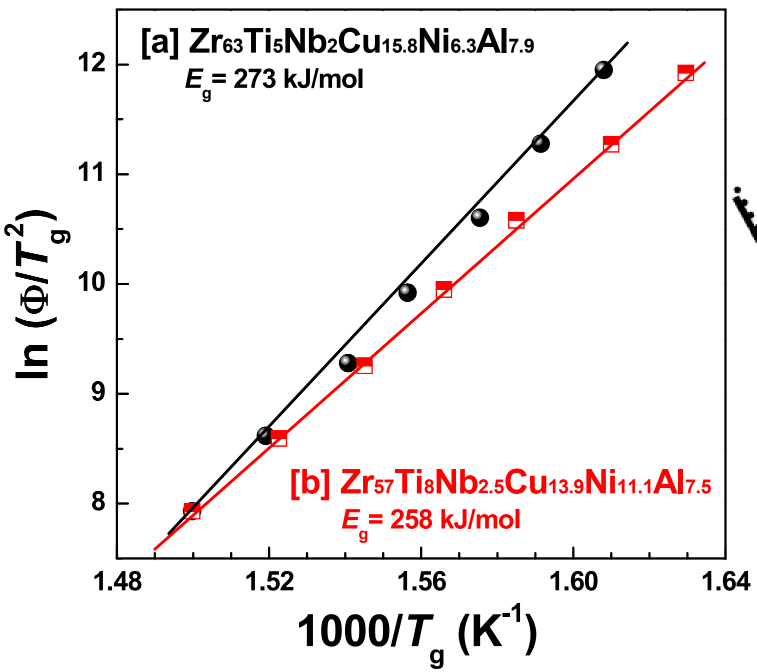

Kissinger's equation

$$\ln(\Phi / T_g^2) = -Q / RT_g + const.$$

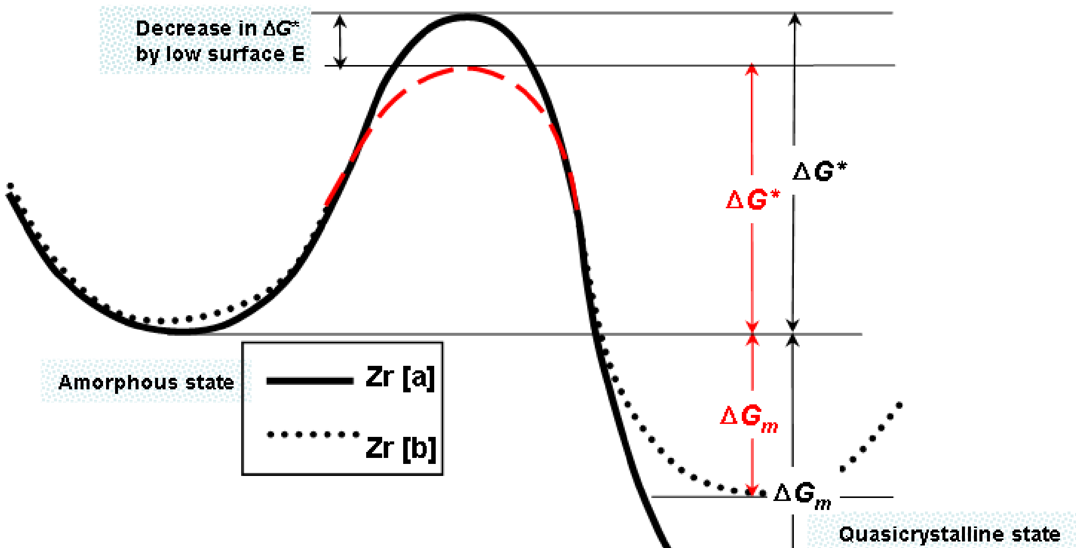

Nucleation rate

$$I = A \cdot \exp(-\Delta G^* / kT)$$

Effect of quenched-in quasicrystal nuclei

- Isotherm in DSC

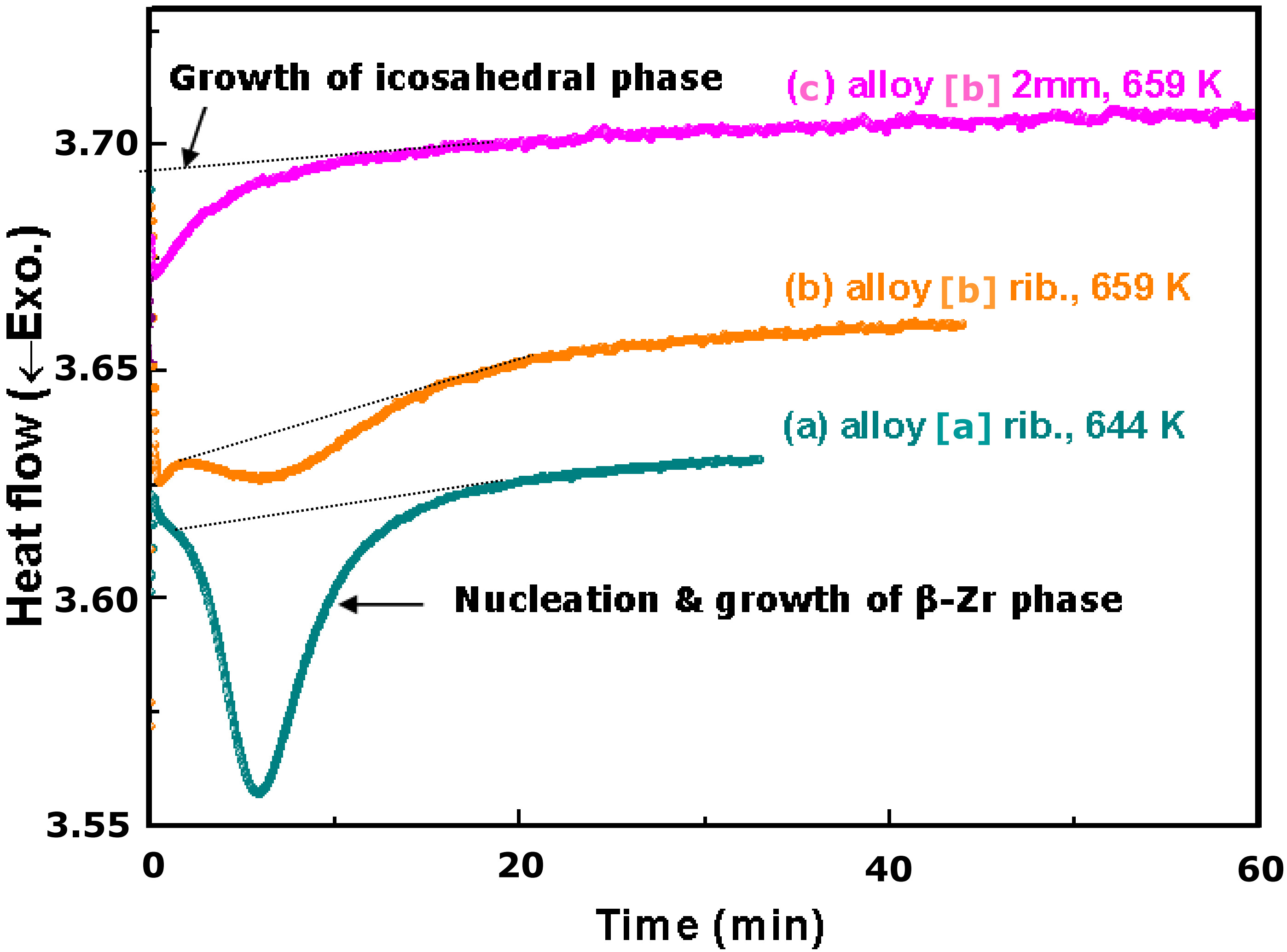

Effect of quenched-in quasicrystal nuclei

- **EXAFS analysis**

(b) $Zr_{57}Ti_8Nb_{2.5}Cu_{13.9}Ni_{11.1}Al_{7.5}$

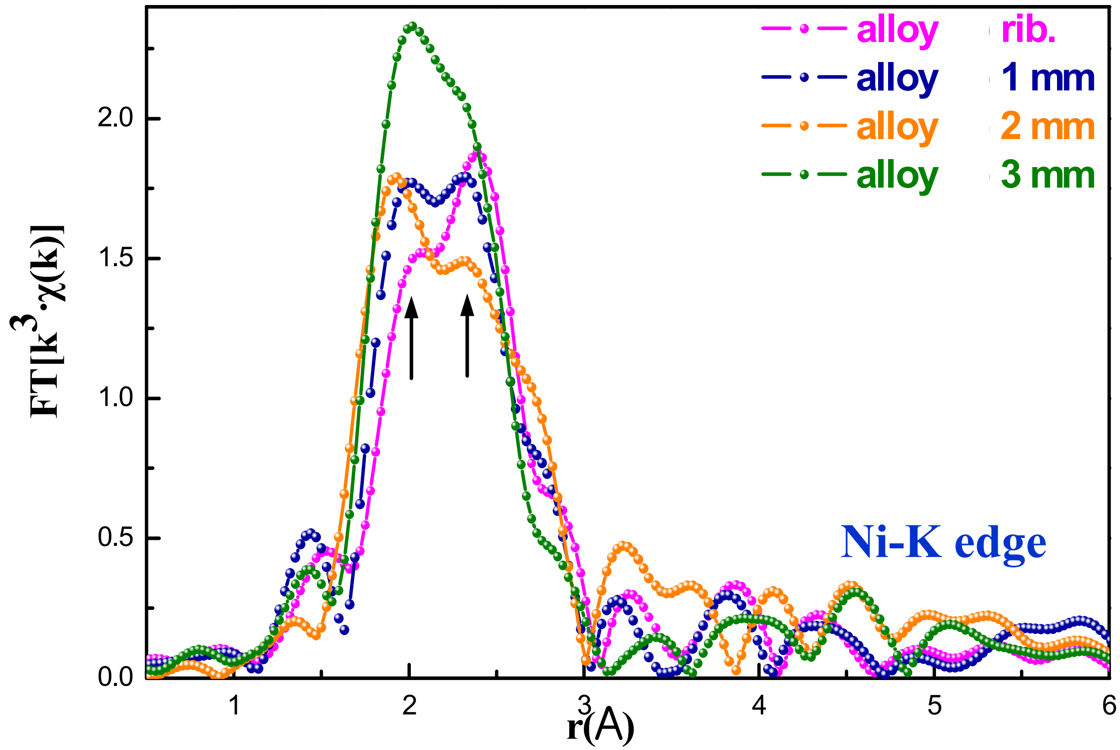

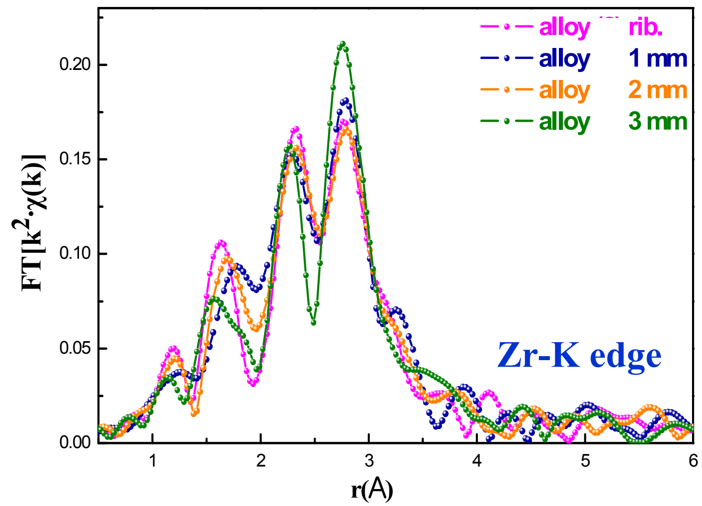

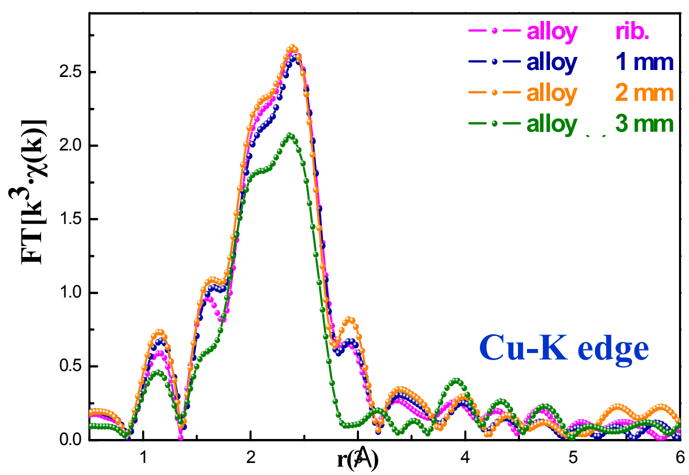

Distinctive structural change around Ni atom

Intensity change due to microstructural change

* unpublished (2008)

Enhancement plasticity in BMGs with atomic scale heterogeneity

b) Effect of element having positive enthalpy of mixing among constituent elements

Improvement of plasticity in monolithic BMGs

*** Enhancement of plasticity in monolithic BMGs**

➡ No clear explanations so far.

*** Reports for enhancement of plasticity in monolithic BMGs**

	Compressive plastic strain, ε_p (%)
$Zr_{59}Ta_5Cu_{18}Ni_8Al_{10}$ [1]	~ 6.1
$Zr_{57}Ti_5Cu_{20}Ni_8Al_{10}$	~ 1.1
$Ni_{59}Zr_{16}Nb_7Ti_{13}Si_3Sn_2$ [2]	~ 6.2
$Ni_{59}Zr_{20}Ti_{16}Si_2Sn_3$	~ 2.1
$Cu_{47}Ti_{33}Zr_7Nb_4Ni_8Si_1$ [3]	~ 4.1
$Cu_{47}Ti_{33}Zr_{11}Ni_8Si_1$	~ 1.5
$Cu_{43}Ag_7Zr_{43}Al_7$ [4]	~ 4.1
$Cu_{50}Zr_{43}Al_7$	~ 1.5

1 *Xing et al., Phys. Rev. B (2001)*

2 *Lee et al., Intermetalics (2004), BMG III*

3 *Park et al., J. Non-cryst. Sol. (2005)*

4 *Sung et al., Met. Mater. –Int (2004) and Oh et al., Scripta Mater. (2005)*

(Ta-Zr: +13KJ/mol, Nb-Zr: +17KJ/mol, Nb-Ti: +9KJ/mol,Cu-Ag: +5 KJ/mol)

- Previous results on the effect of micro-alloying on plasticity

: **Effect of elements having positive heat of mixing**

Alloy design

* Substitution of Zr with Y in Cu-Zr-Al system

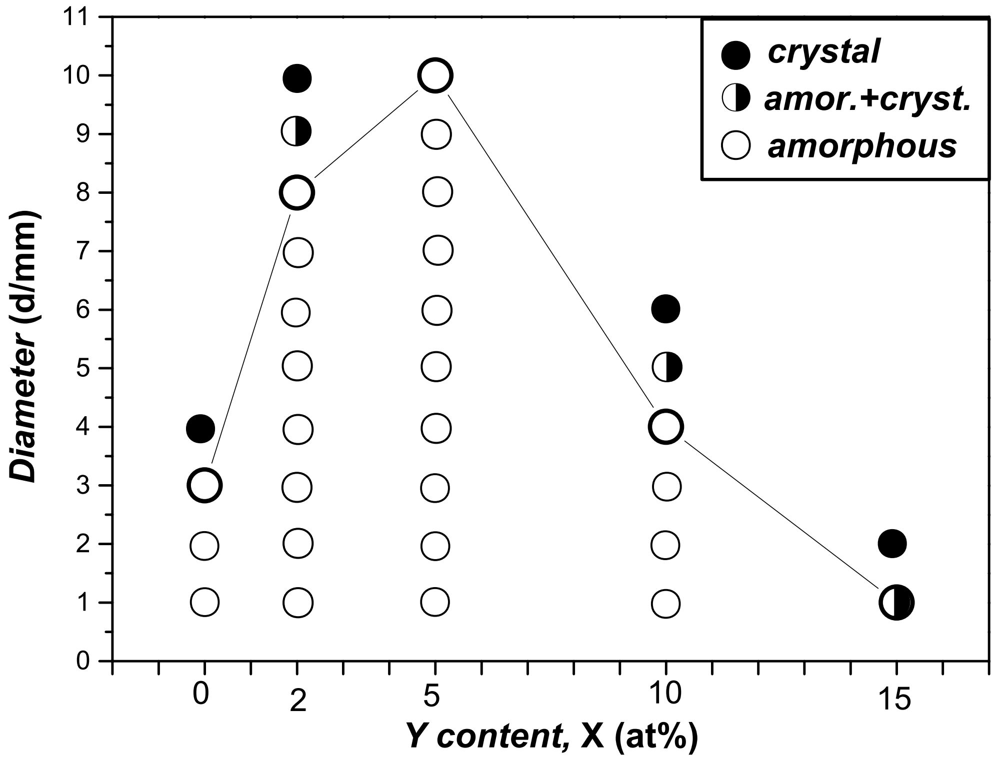

D. Xu, G. Duan and W.L. Johnson, Phys. Rev. Lett. 92, 245504 (2004)

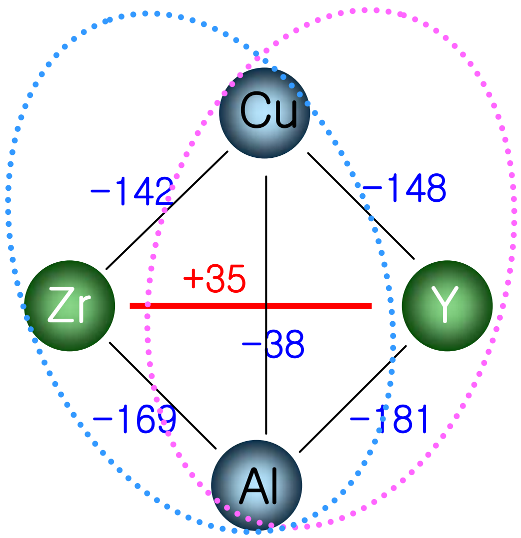

Possibility of two phase !!!

→ **Cu-Zr-Al , Cu-Y-Al**

Indirect evidence of inhomogeneity
= Phase separation

*** Acta Materialia, 54, 2597 (2006)**

Thermal analysis : DSC results

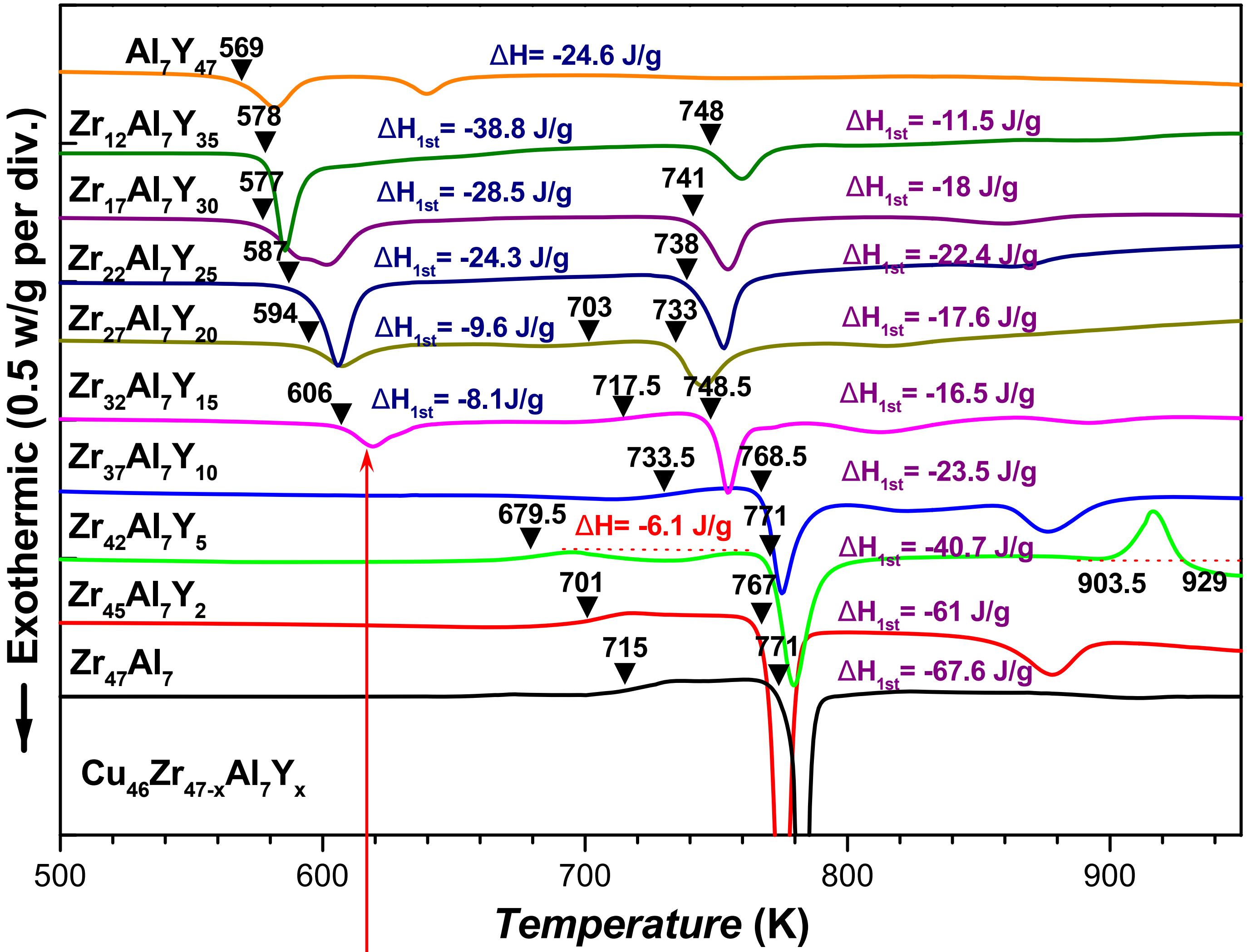

Exothermic peak which exhibit that Y rich amorphous phase crystallize

Structural analyses : TEM results

As-melt-spun

- With increasing Y content,
  Compositional inhomogeniety → Phase separation

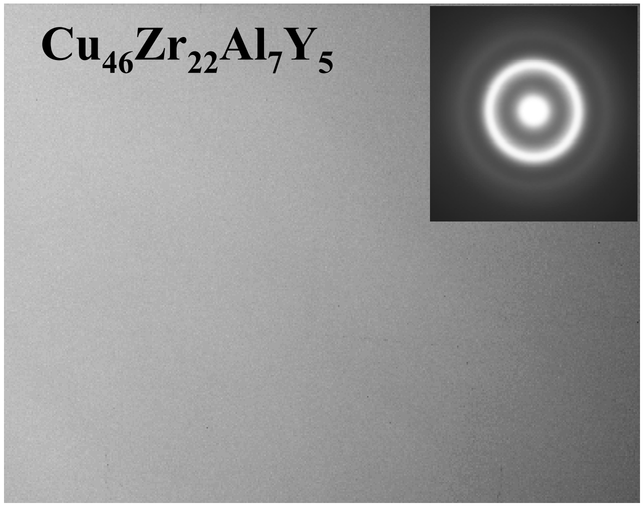

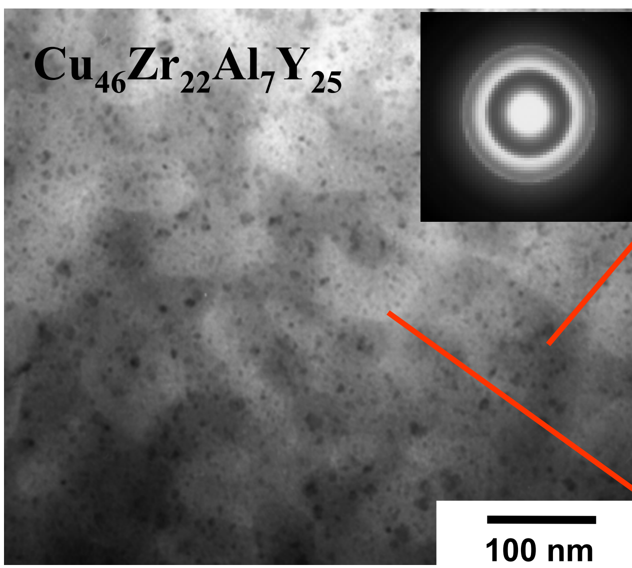

$Cu_{53.4}Zr_{31.8}Y_{8.3}Al_{6.5}$ (CuZr-rich)

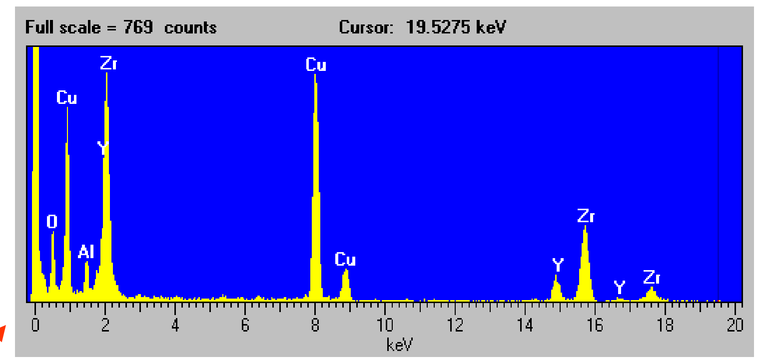

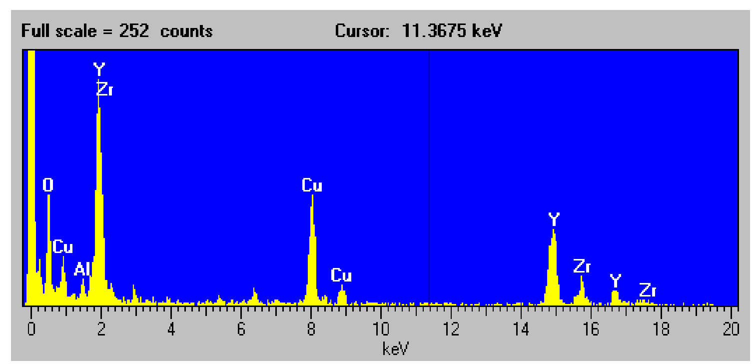

$Cu_{35.7}Zr_{12.8}Y_{44.3}Al_{7.2}$ (CuY-rich)

Compression test in Cu-Zr-Al-Y alloy system

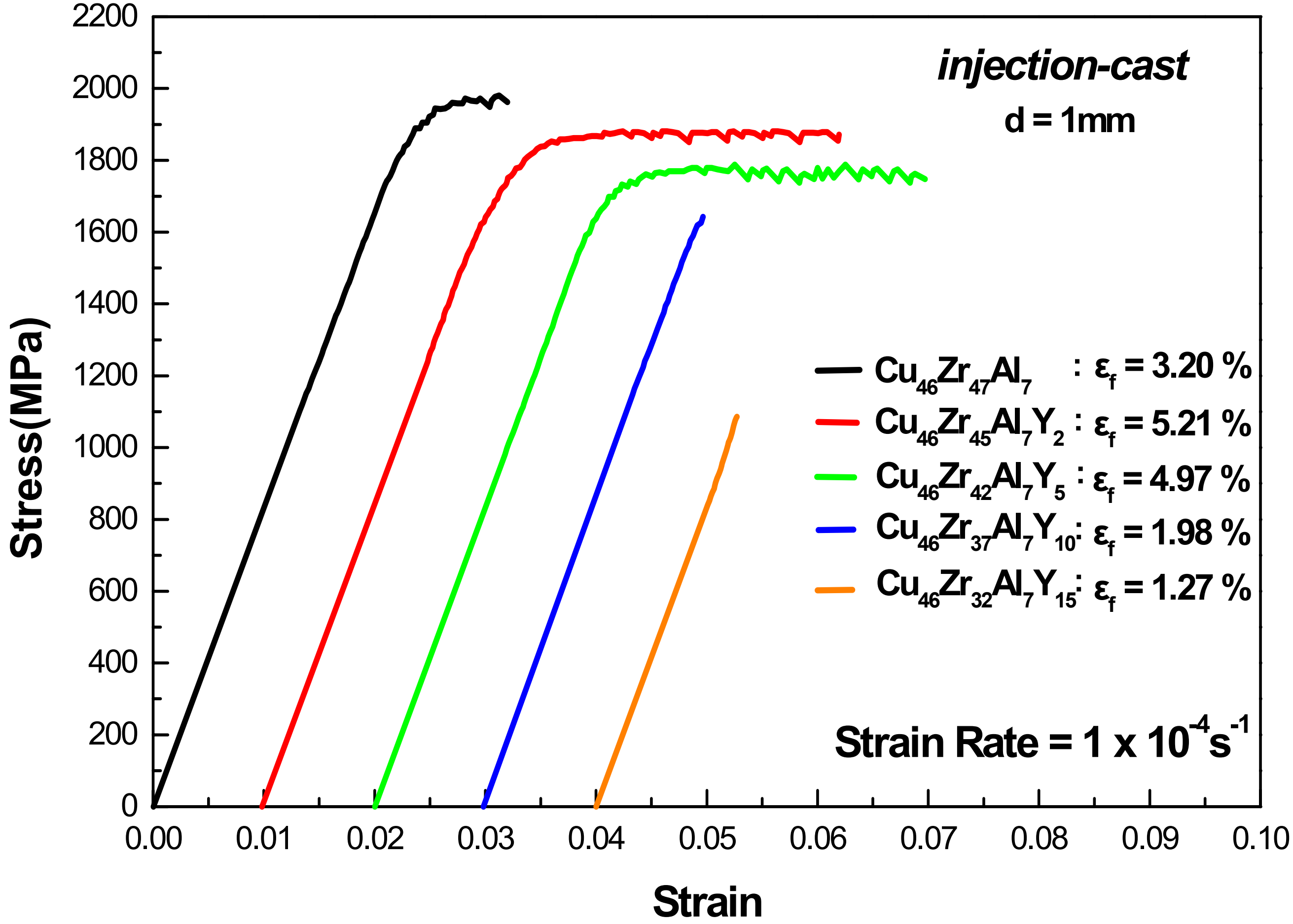

⇒ Enhancement of the plasticity with the addition of small amount (2~5 %) of Y

But, no nanocrystals and structural ordering (conformed by HREM and HRND)

Performed at ***HANARO, KEARI***.

Calculation of activation energy for glass transition

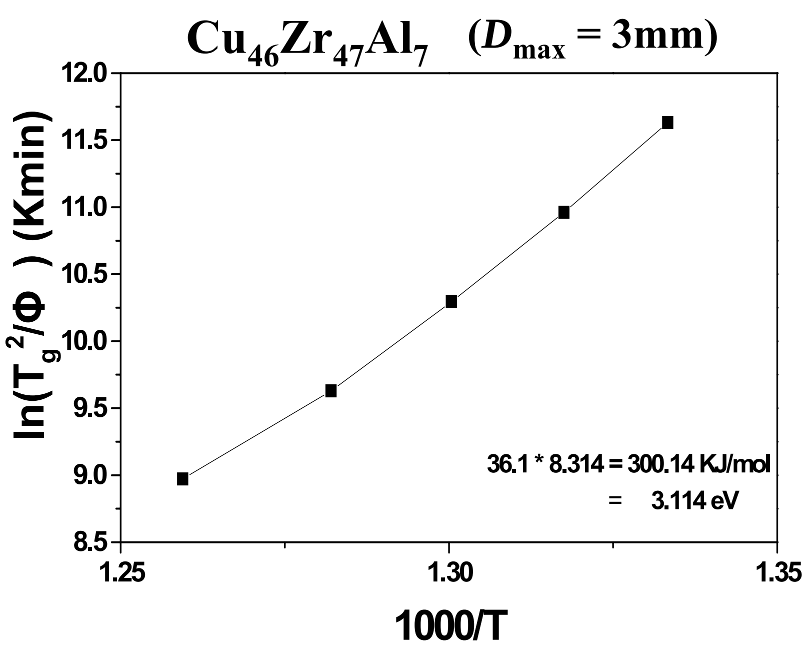

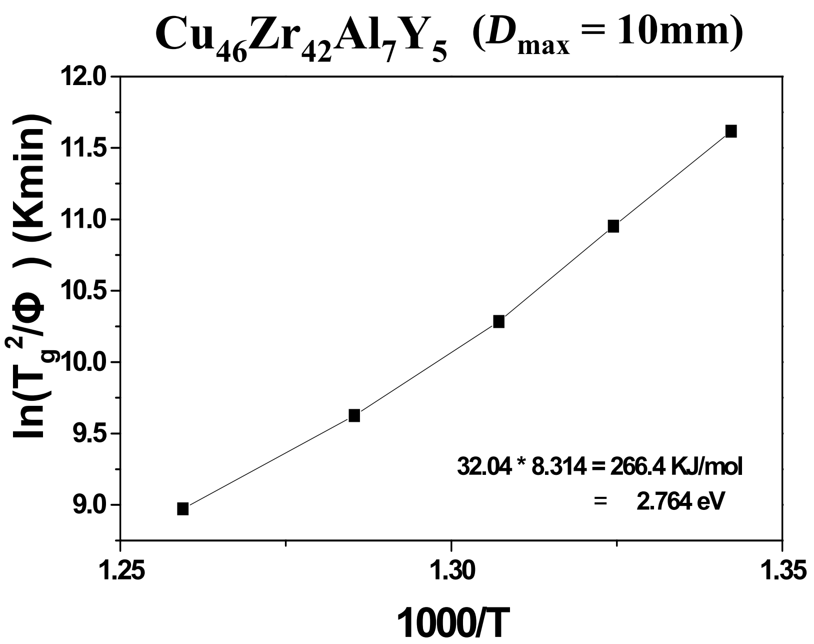

- **activation energy** evaluated by Kissinger's equation;

$$\ln (T_g^2/\Phi) = \ln (E_g/k_B K_0) + E_g/k_B T_g,$$

where k_B is the Boltzman constant, and K_0 is the frequency factor in Arrehenius law, that is, $K_T = K_0 \exp(-E/k_B T)$.

* E_g = 3.114 eV > * E_g = 2.764 eV

Relatively stable glass

Measurement of viscosity using TMA

<Supercooled liquid region>

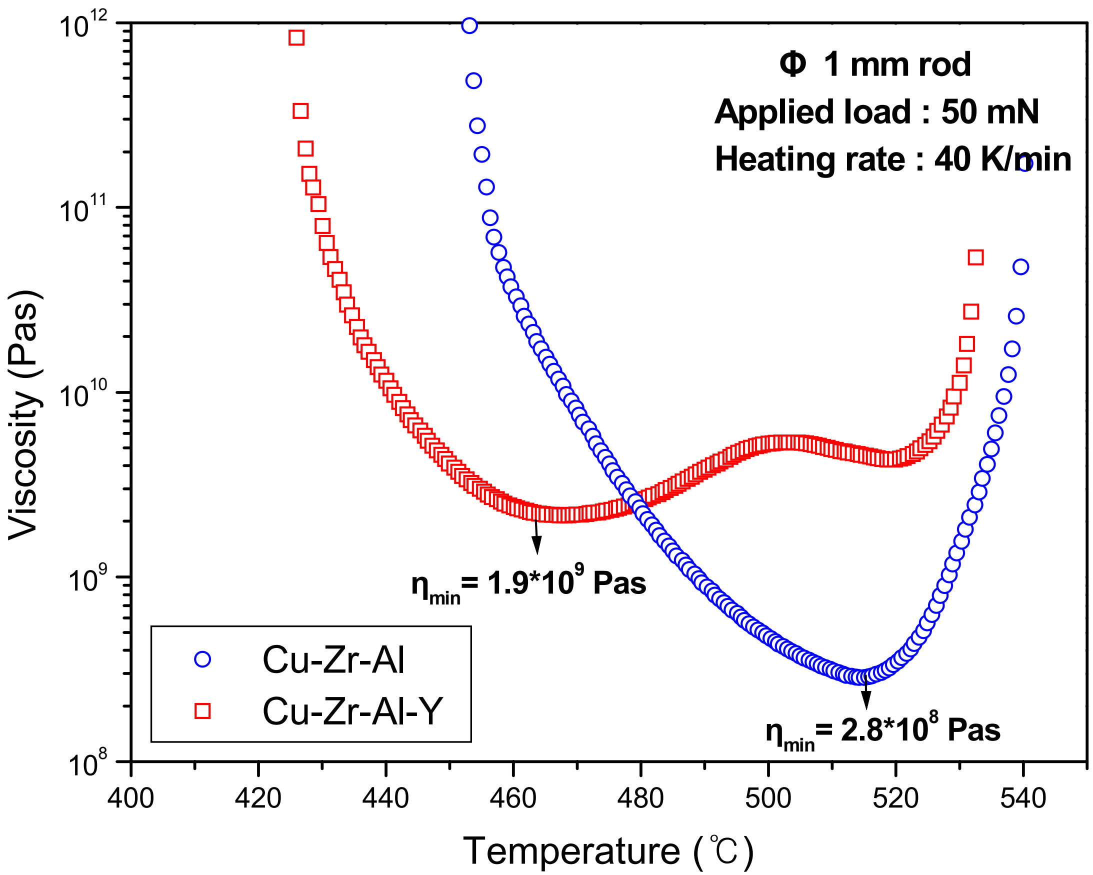

<1st Crystallization behavior>

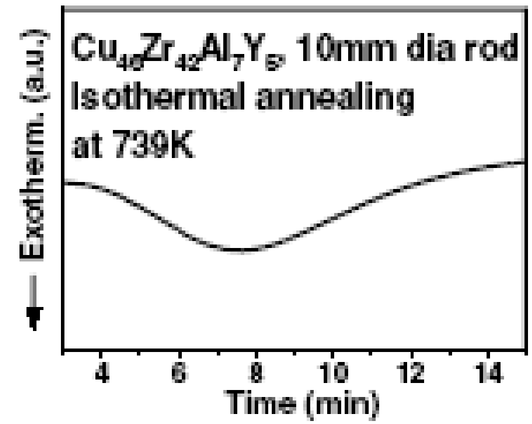

: nucleation and growth

$Cu_{46}Zr_{47}Al_7$ < $Cu_{46}Zr_{42}Al_7Y_5$

η_{min} **= 2.8*10^8 pas**

η_{min} **= 1.9*10^9 pas**

Relatively easy crystallization

Structural analyses: HRTEM

$Cu_{46}Zr_{42}Al_7Y_5$

As-melt-spun

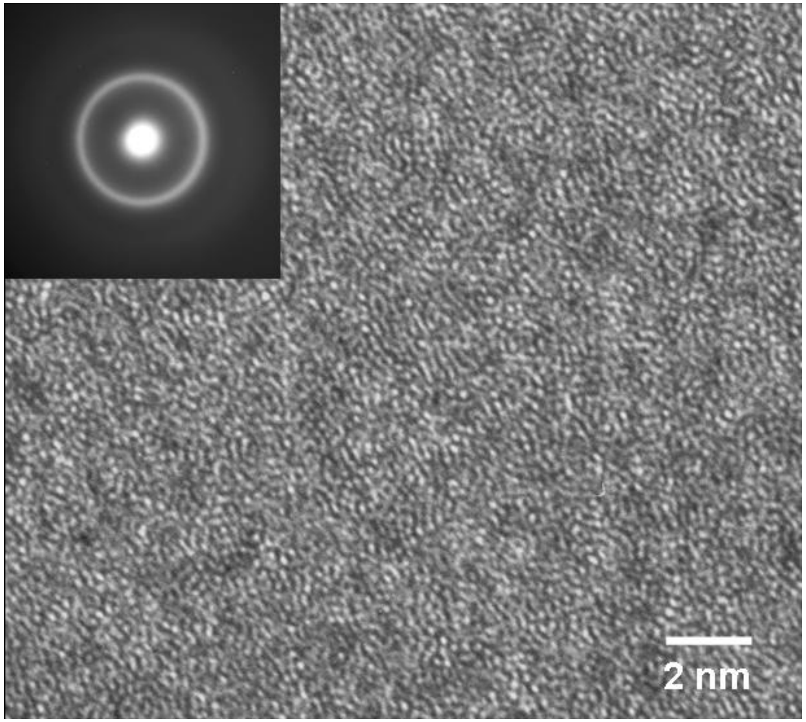

Heated up to 480℃

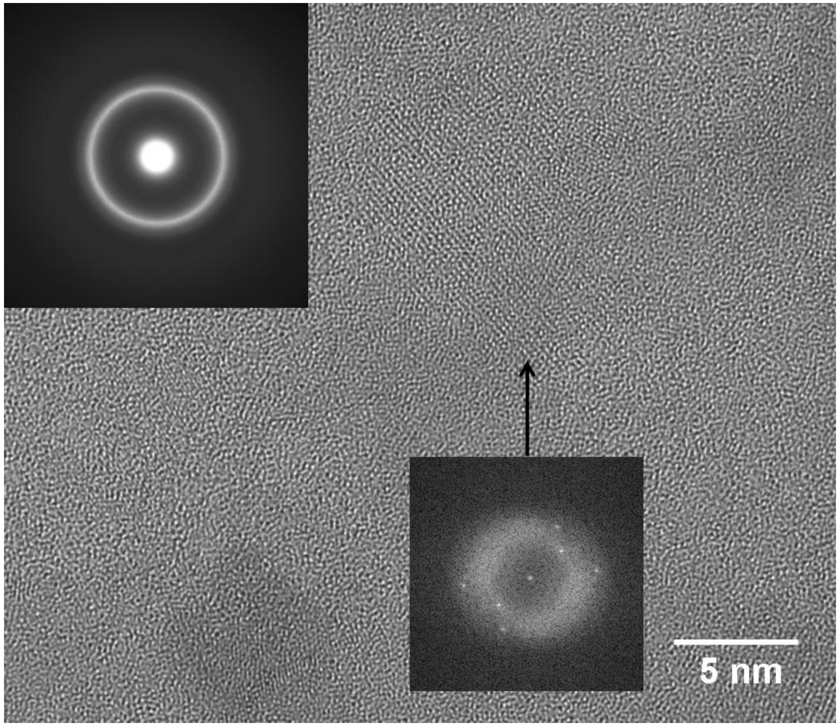

: nanocrystallization of Y rich amorphous phase due to relatively lower GFA

* Acta Materialia, 54, 2597 (2006)

Calculation of kinetic fragility, m

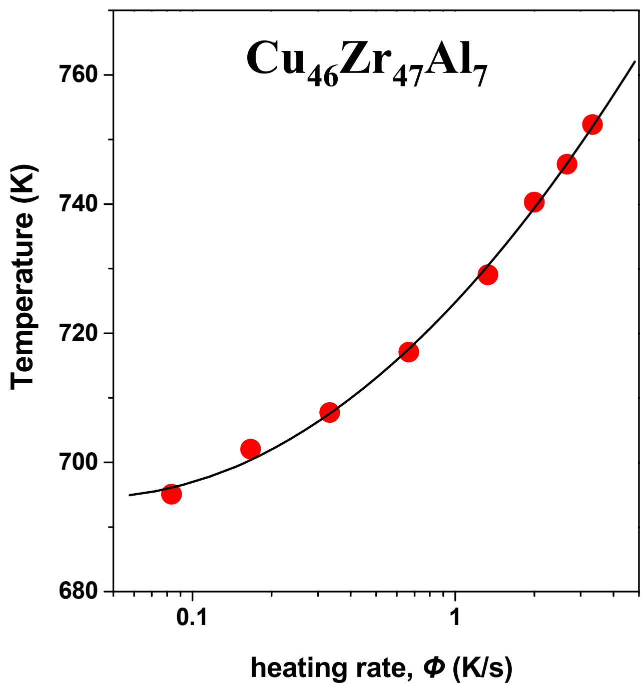

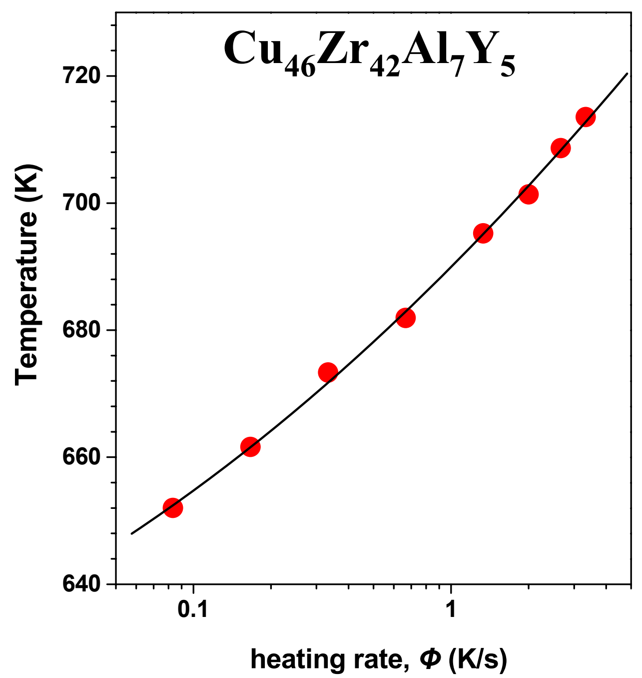

the relationship of T_g and ln Φ with the Vogel-Fulcher (VF) equation:

$\ln \Phi = \ln B - D^* T_g^0/(T_g - T_g^0)$,

where B is a constant, T_g^0 is the hypothetical kinetic instability point which is a lower limit of T_g, that is, the VF temperature, and D* is the strength parameter which can be used to describe how closely the system obeys the Arrhenius law.

*** Least Squares Fitting**

$$m = \left.\frac{d \log \eta(T)}{d(T_{g,n}/T)}\right|_{T=T_{g,n}} = \left.\frac{d \log \tau(T)}{d(T_g/T)}\right|_{T=T_g}$$

$$m = [D^* T_g^0\, T_g]/[\ln 10 (T_g - T_g^0)^2]$$

Heating rate : 5 K/min

ln A = 8.74
T_g^0 = 640 K
D^* = 0.61

25

Relatively strong glass

ln A = 14.2
T_g^0 = 502 K
D^* = 3.78

40

Relatively fragile glass

Effect of element having positive enthalpy of mixing

- **Abnormal behavior of supercooled liquid region**

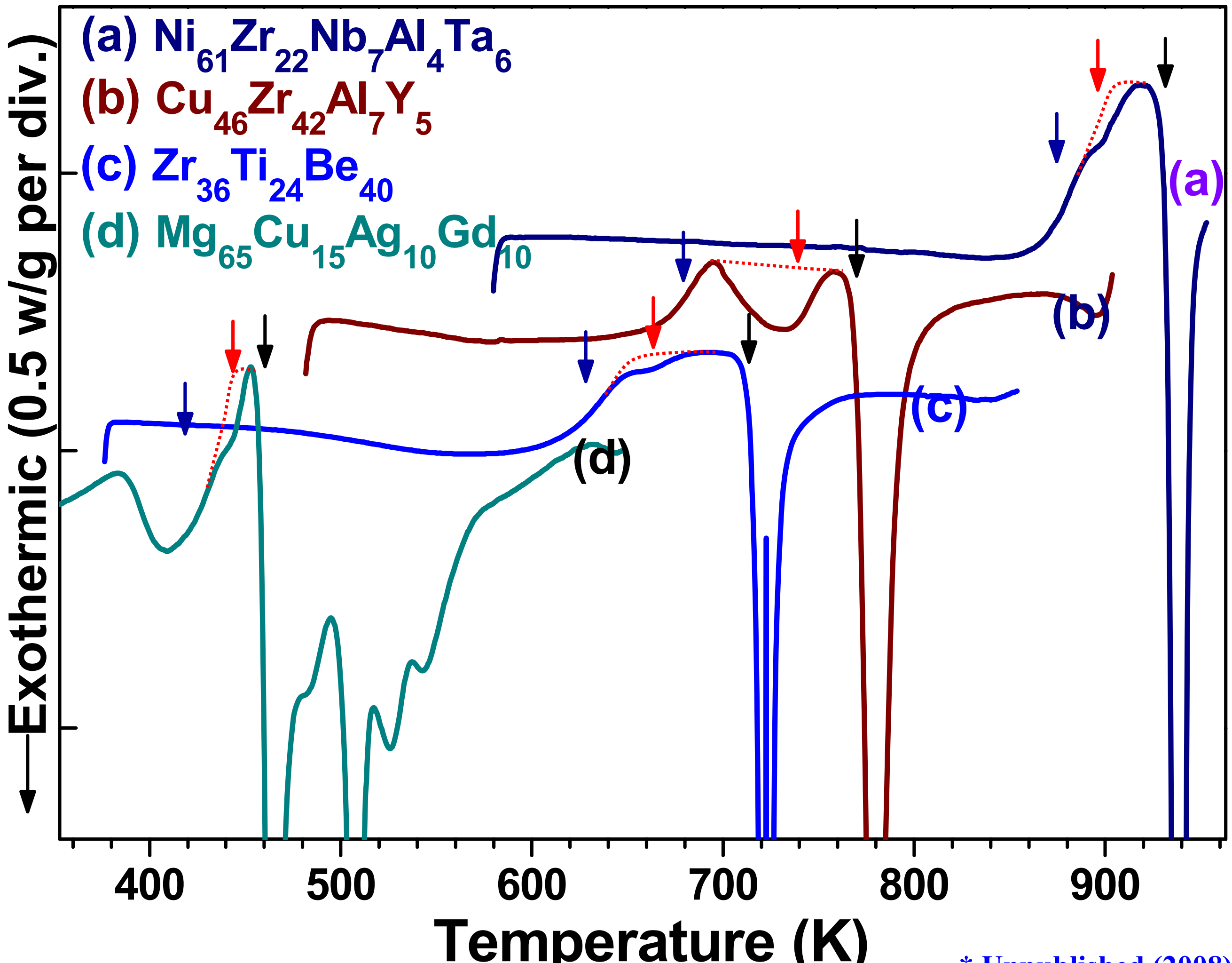

* Unpublished (2008).

Effect of element having positive enthalpy of mixing

- **Atom probe concentration depth profiles in $Ni_{61}Zr_{22}Nb_{7}Al_{4}Ta_{6}$**

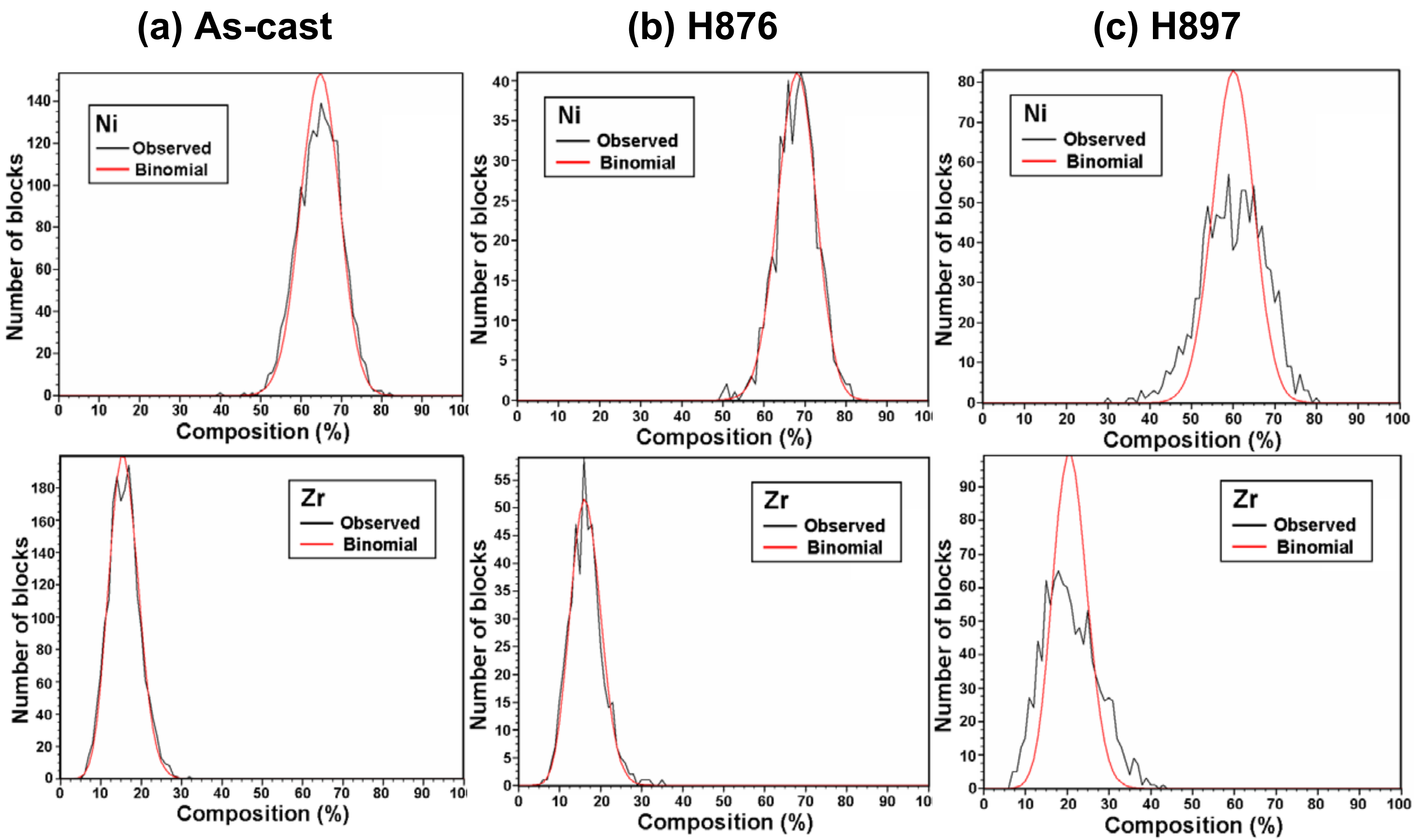

easy crystallization

Effect of element having positive enthalpy of mixing

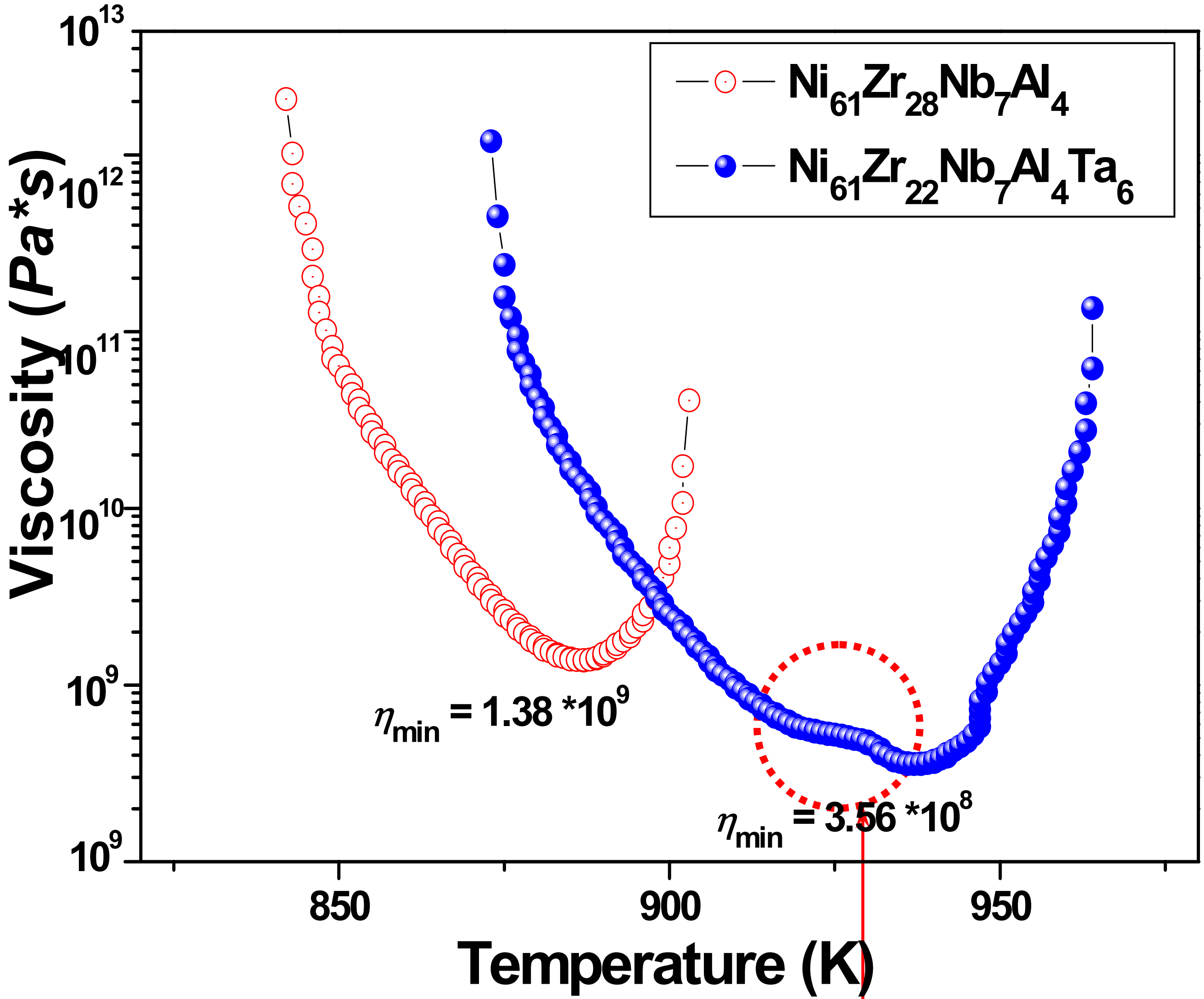

Ordering in supercooled liquid region

Enhancement plasticity in BMGs with atomic scale heterogeneity

c) Effect of element having significantly different enthalpy of mixing among constituent elements

Effect of element having large different enthalpy of mixing

- **Cu-Zr-Be ternary alloy system**

* Acta Materialia, 56 3120 (2008)

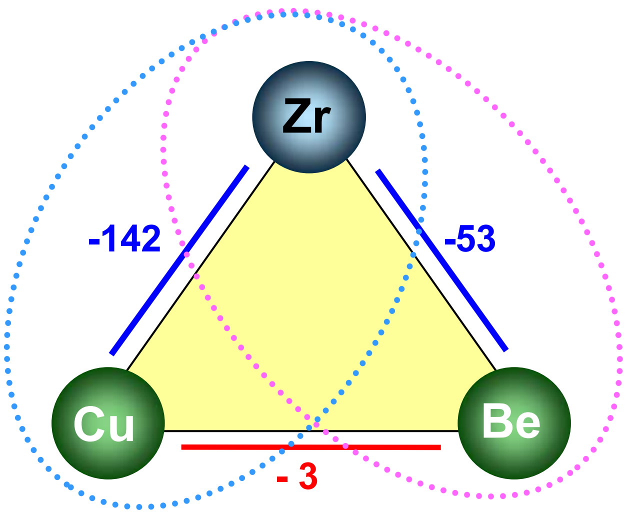

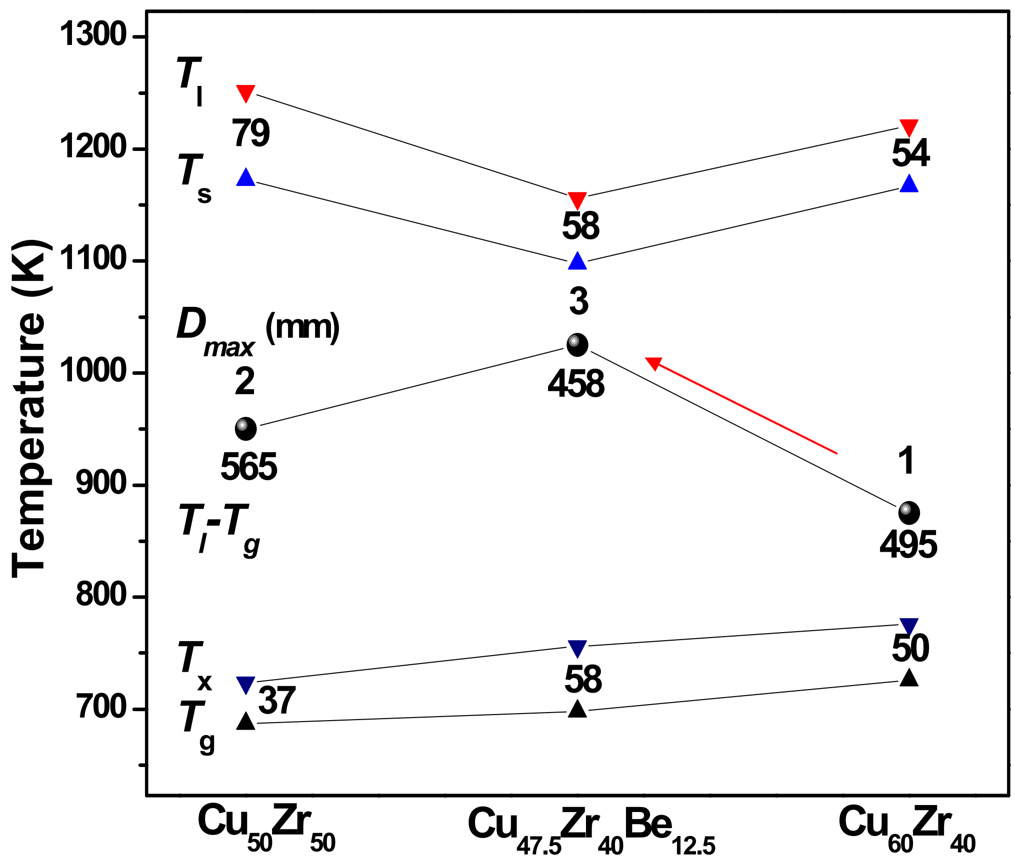

Effect of element having large different enthalpy of mixing

- Compression test

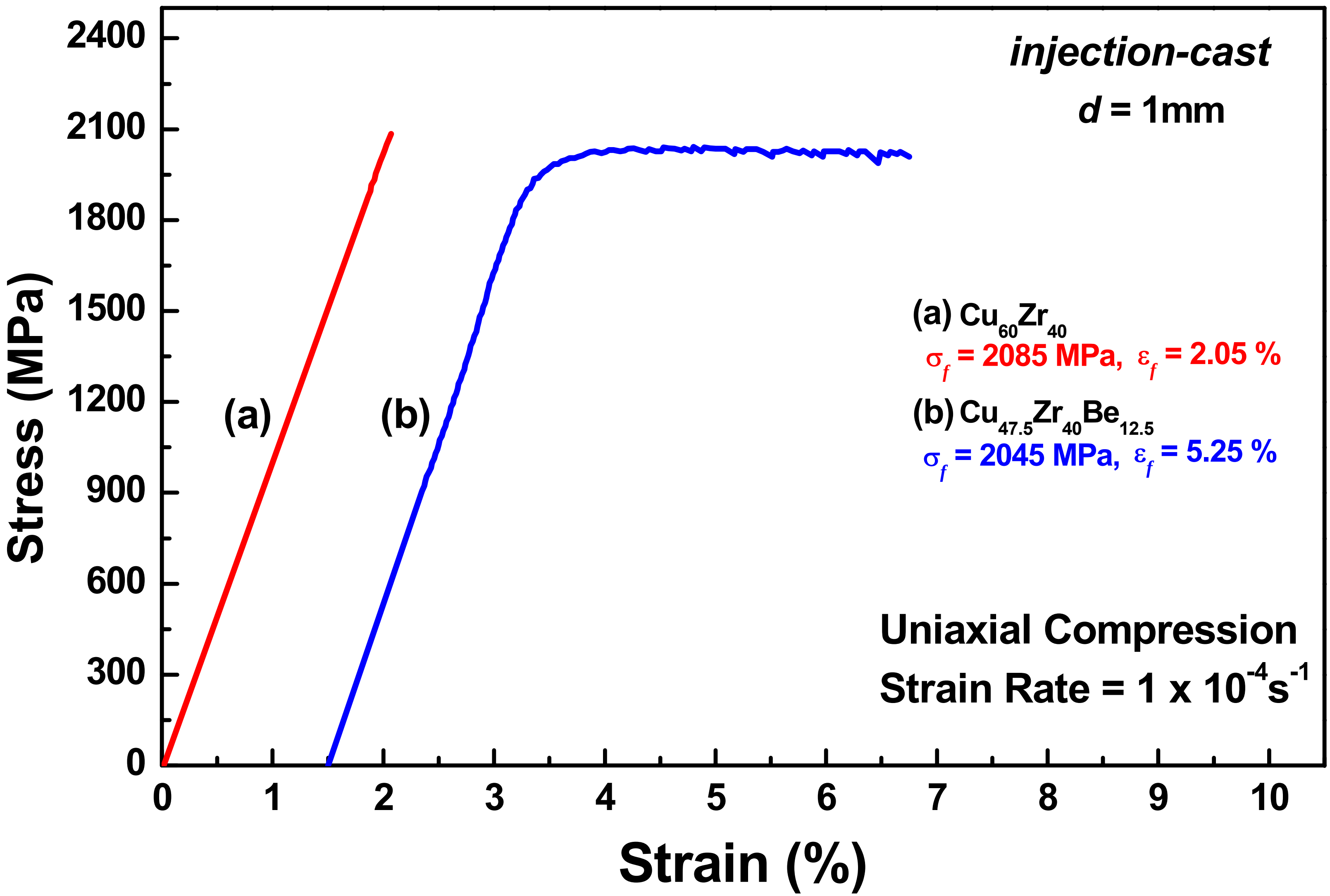

Effect of element having large different enthalpy of mixing

- **3DAP-FIM results**

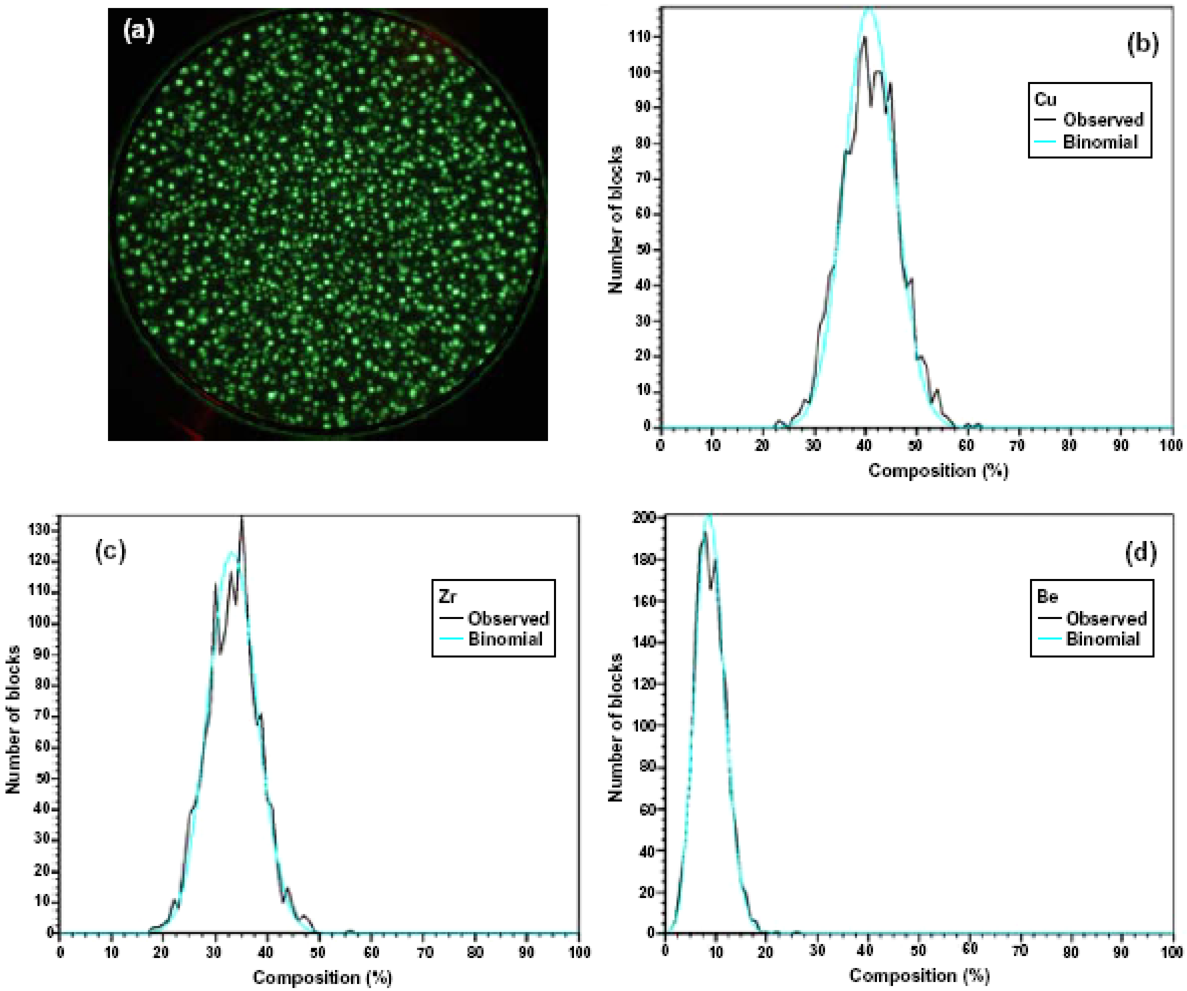

(a) FIM image and (b)-(d) composition depth profile of the as-spun $Cu_{47.5}Zr_{40}Be_{12.5}$ ribbon sample

Visualization of Atoms by FIM

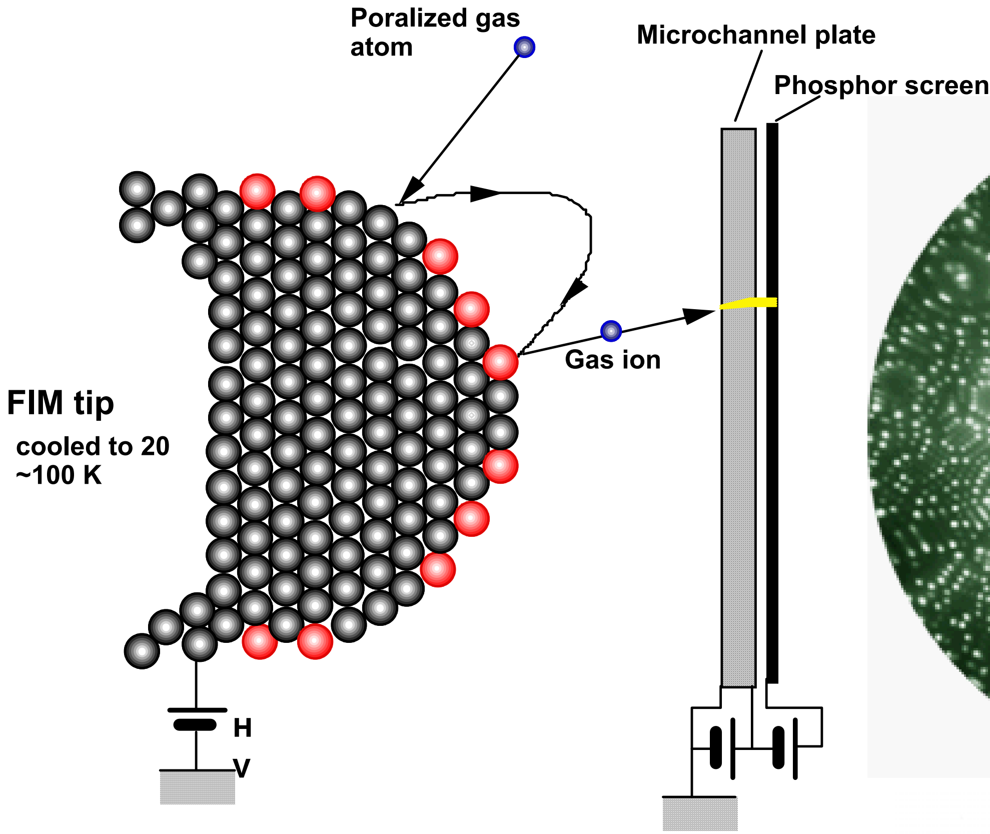

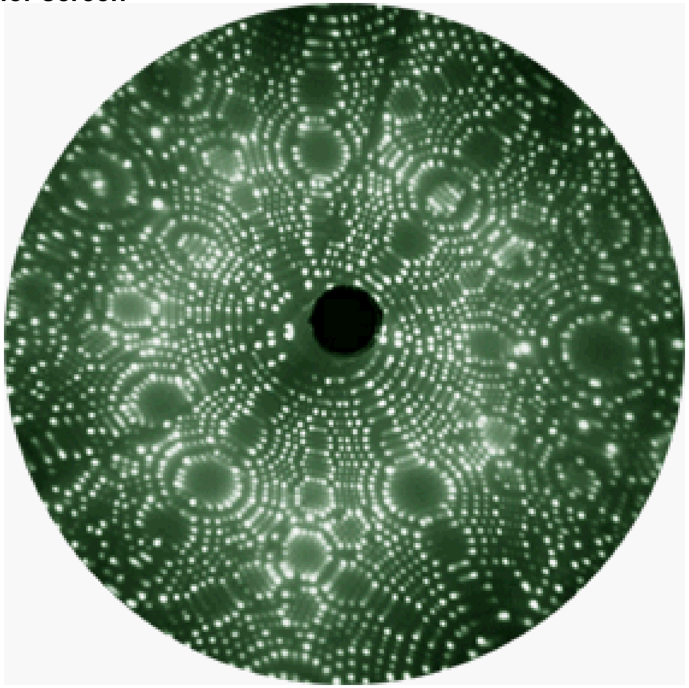

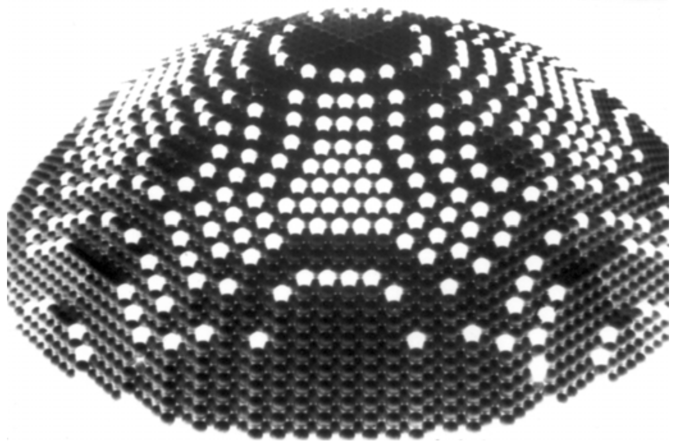

Analysis of atoms by 3DAP

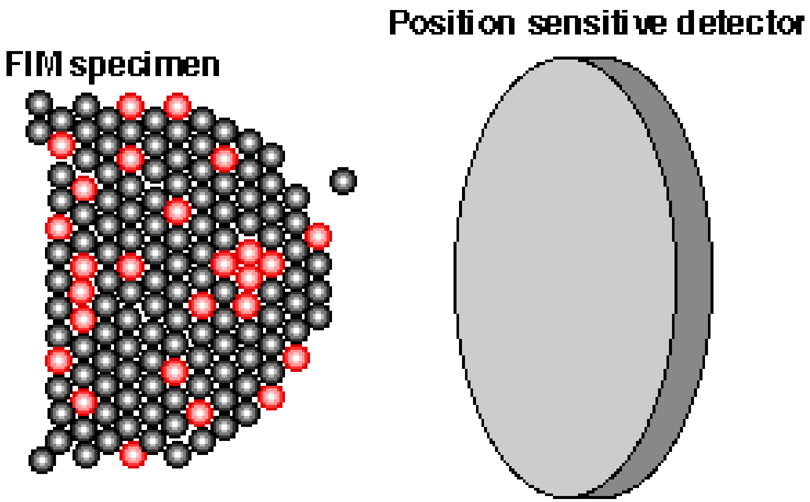

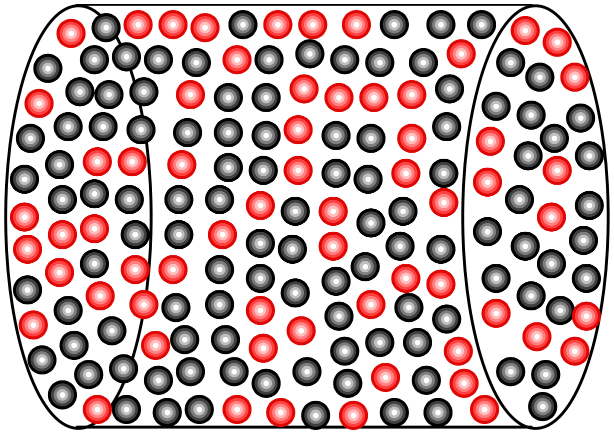

η' precipitates in Al-Zn-Mg alloy

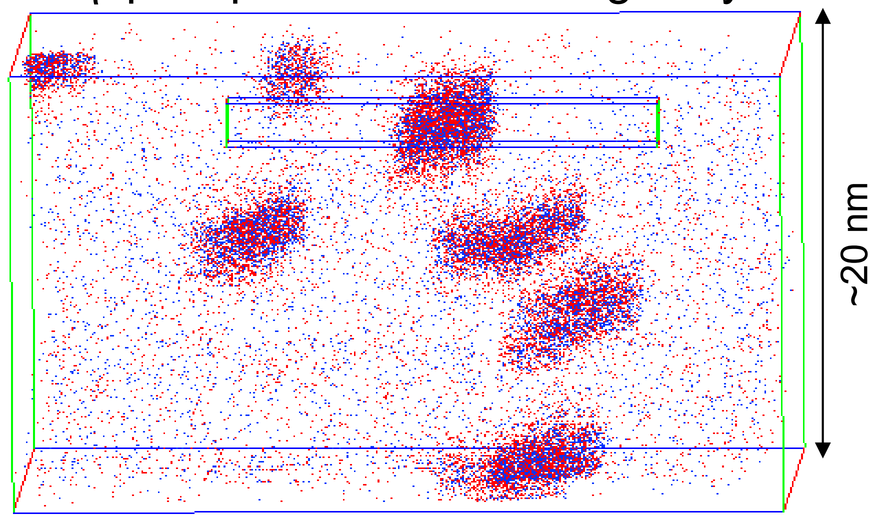

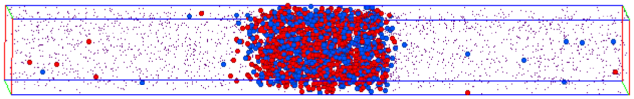

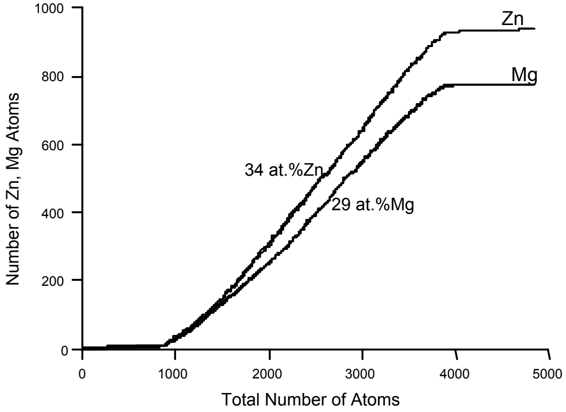

Energy-compensating reflectron lens

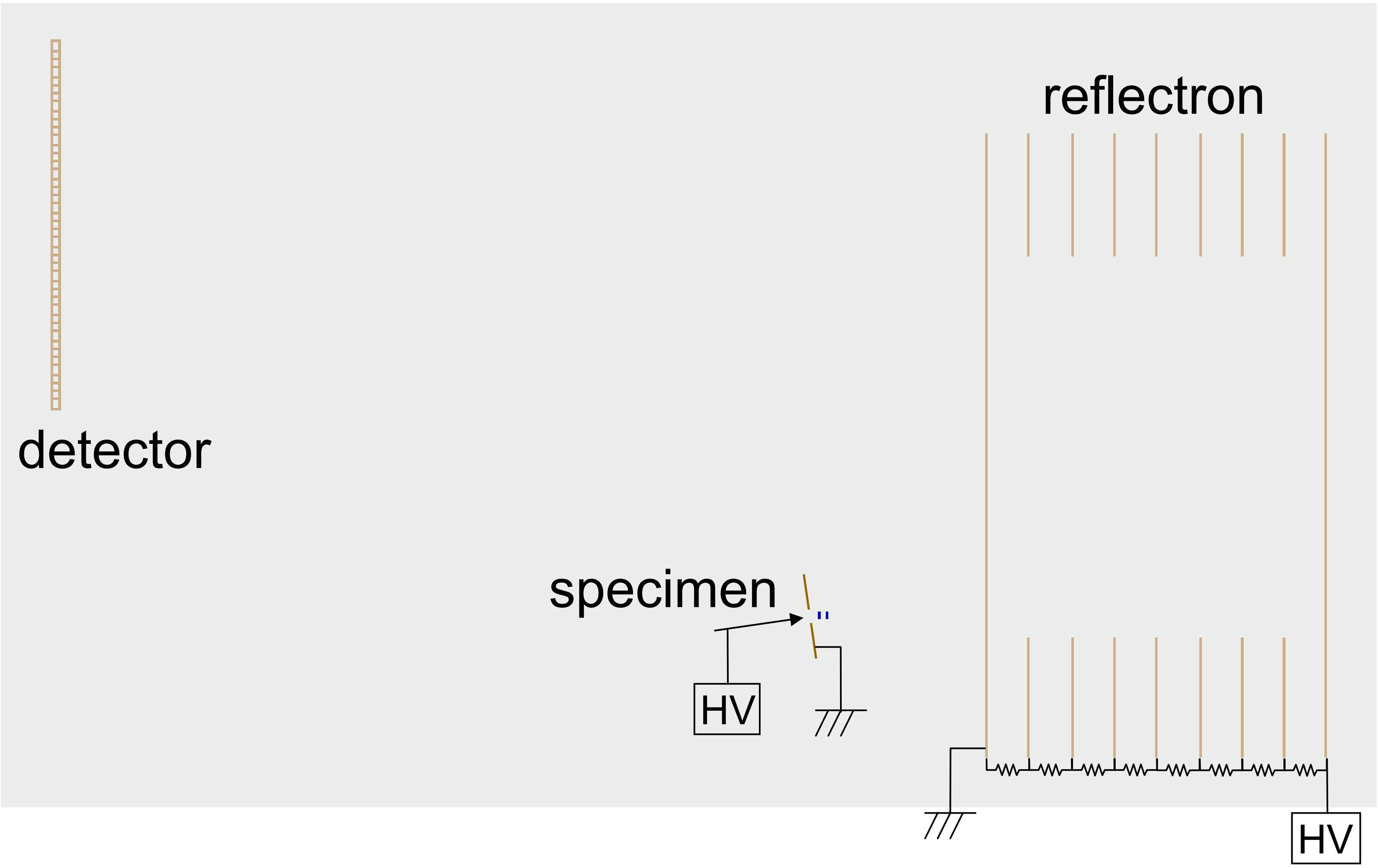

NIMS 3DAP

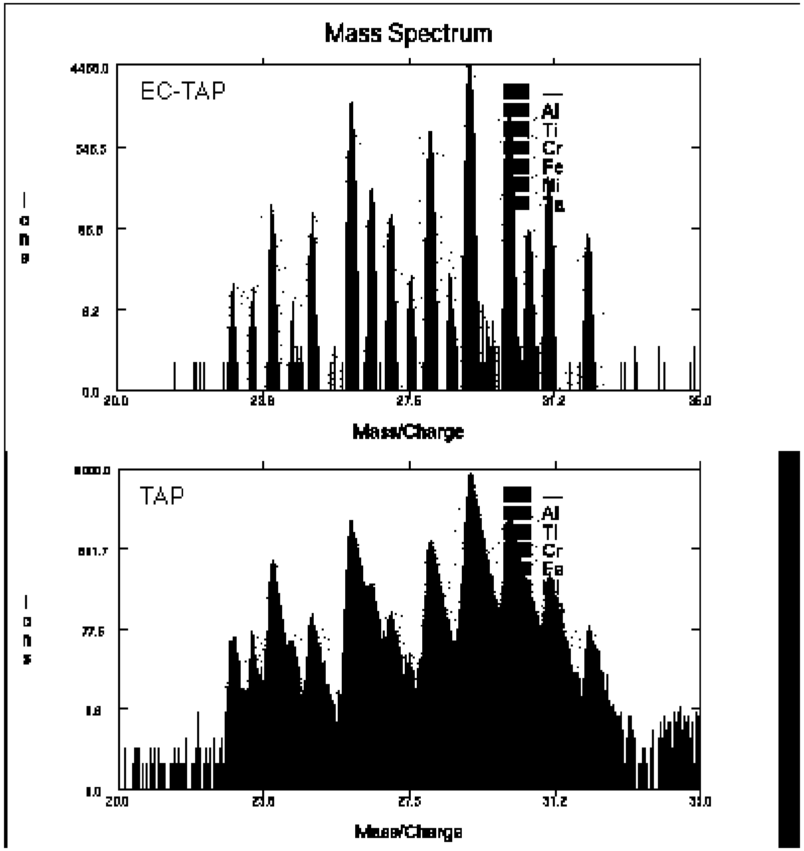

Mass Spectrum
EC-TAP
Al
Ti
Cr
Fe
Ni
Mass/Charge
TAP
Al
Ti
Cr
Fe
Mass/Charge

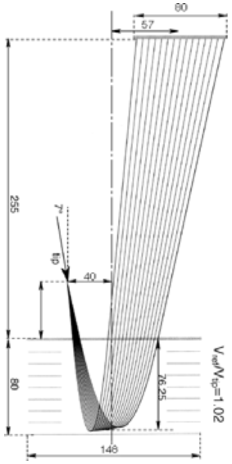

60
57
255
tip
40
80
76.25
146

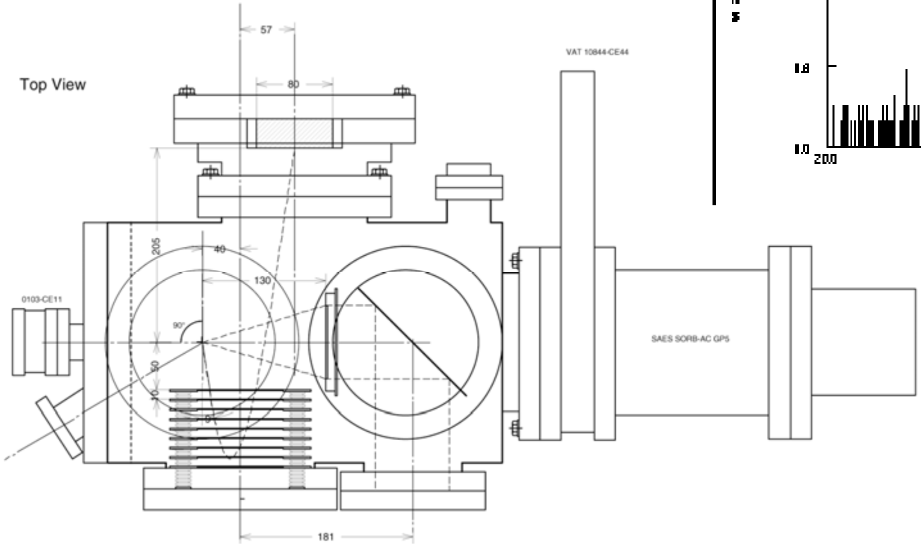

Top View
57
80
VAT 10844-CE44
0103-CE11
40
130
SAES SORB-AC GP5
181

Complementary structural analysis

Local Chemical Composition

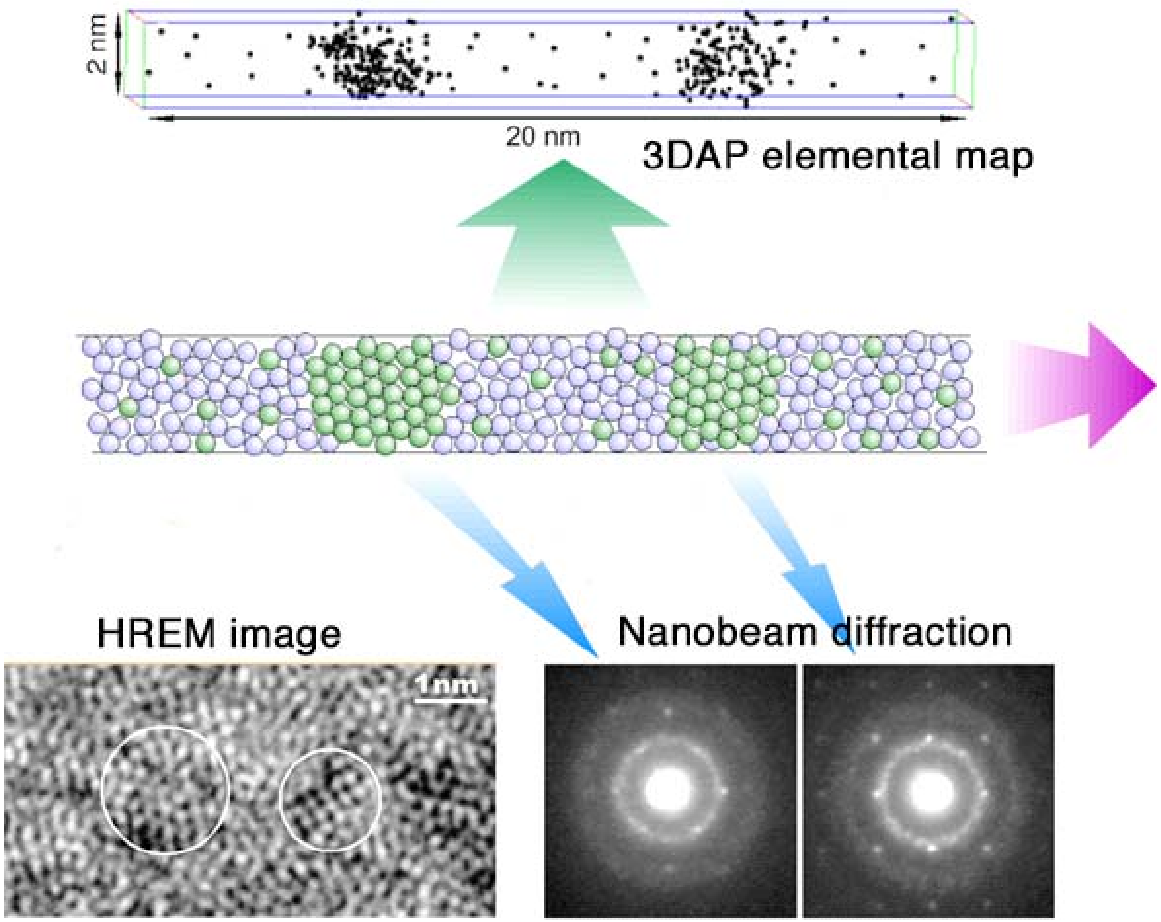

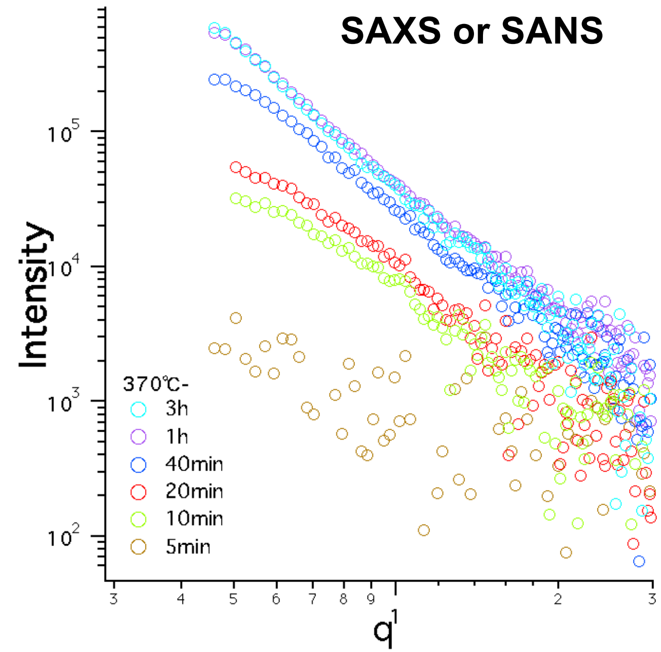

Average Scale

Local Structure

Effect of element having large different enthalpy of mixing

* Acta Materialia, 56 3120 (2008)

EXAFS analysis

	r (Å)		*N*		Total *N*	σ^2	
	Cu-Cu	Cu-Zr	Cu-Cu	Cu-Zr		Cu-Cu	Cu-Zr
$Cu_{60}Zr_{40}$	2.49	2.69	3.0	3.7	6.7	0.0116	0.0233
$Cu_{47.5}Zr_{40}Be_{12.5}$	2.51	2.70	2.5	4.8	7.3	0.0107	0.0227
	Zr-Zr	Zr-Cu	Zr-Zr	Zr-Cu		Zr-Zr	Zr-Cu
$Cu_{60}Zr_{40}$	3.10	2.68	6.9	4.4	11.3	0.0263	0.0124
$Cu_{47.5}Zr_{40}Be_{12.5}$	3.12	2.69	6.2	3.5	9.7	0.0257	0.0130

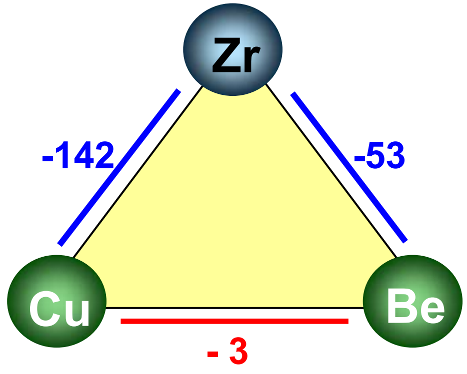

Atoimic diameter in Å: Cu-Cu = 2.56, Cu-Zr = 2.88, Zr-Zr = 3.20.

Cargill-Spaepen short-range order parameters, η

	Z_{AB}	<Z>	Z^*_{AB}	Z^{**}_{AB}	η
$Cu_{60}Zr_{40}$	3.7	8.540	3.416	3.546	0.043
$Cu_{47.5}Zr_{40}Be_{12.5}$	4.8	7.348	2.939	3.855	0.245

Cargill-Spaepen SRO parameter

$$\eta = Z_{AB} / Z^{**}_{AB} - 1$$

$$Z^{**}_{AB} = x_B Z_B Z_A / < Z >$$

$\eta > 0$

chemical ordering between AB nearest-neighbor pairs

Enhancement plasticity in BMGs with atomic scale heterogeneity

d) Effect of atomic scale heterogeneity on SB nucleation

Effect of alloy composition on SB nucleation

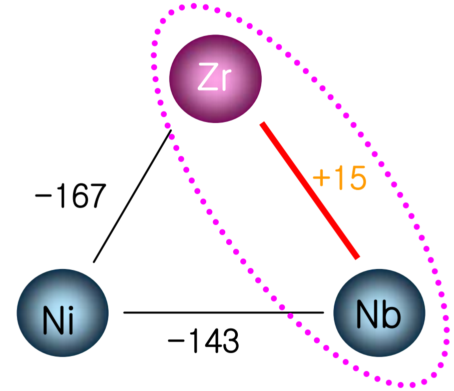

***Ni-Nb-Zr ternary alloy system**

$Ni_{60}Nb_{40}$ and $Ni_{60}Nb_{20}Zr_{20}$ alloys

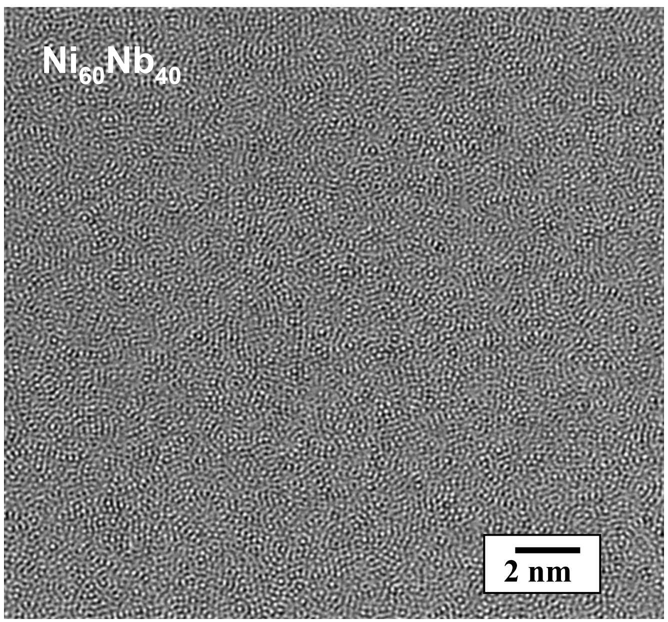

Zr addition

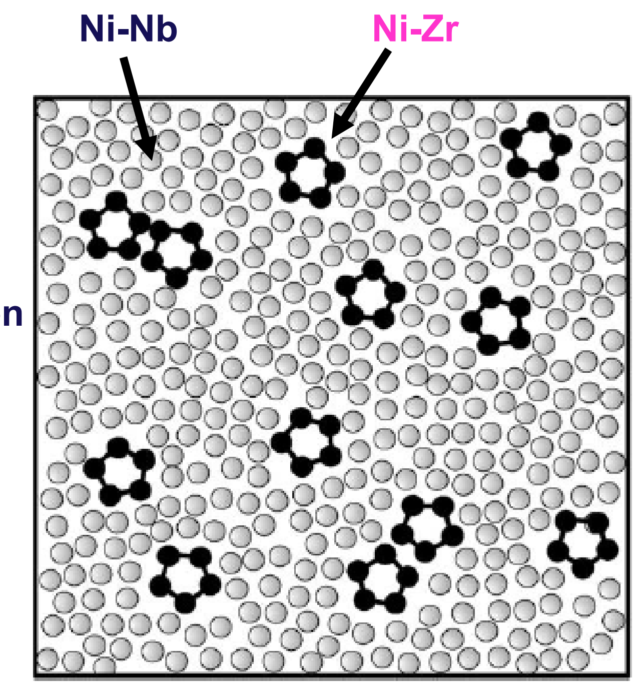

Compositional inhomogeniety

(conformed by EXAFS)

Experimental equipment

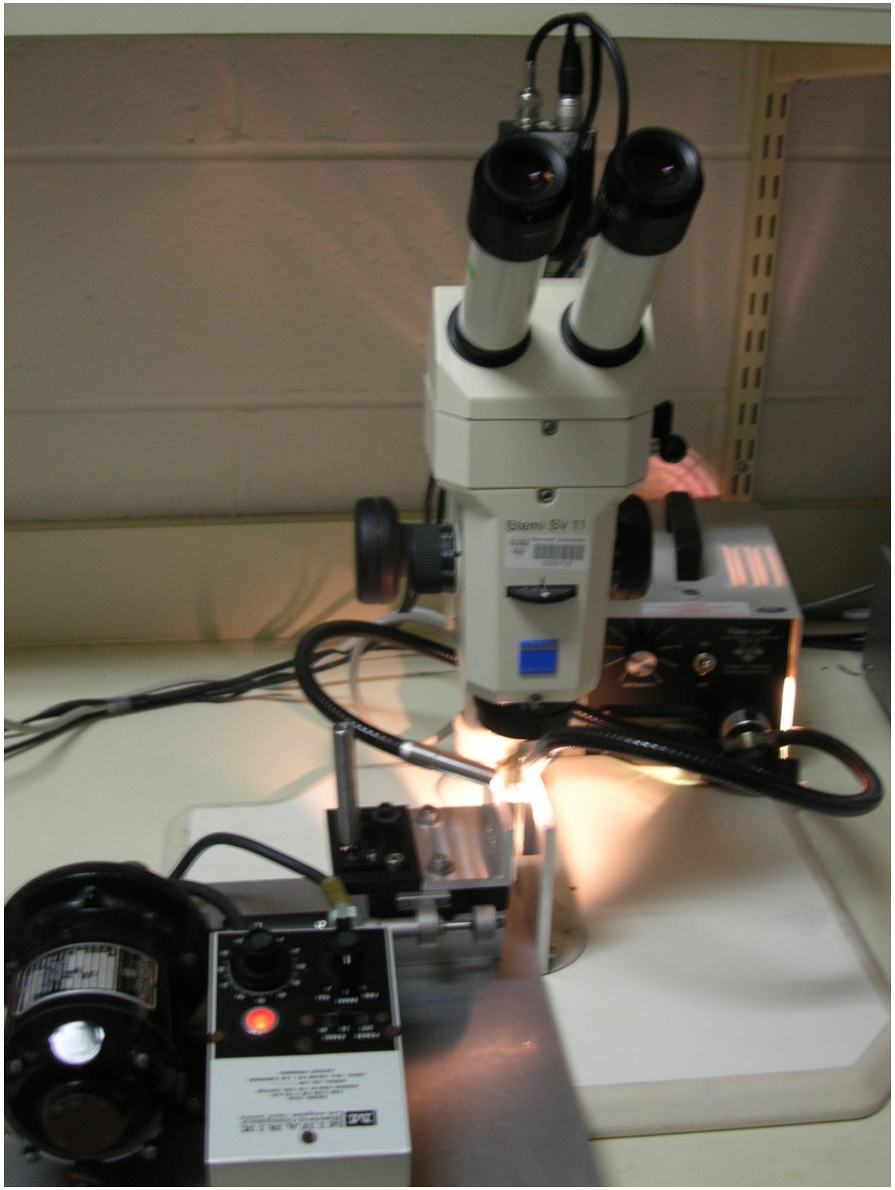

Normal camera
25 frames per sec
Interval : 0.04 sec

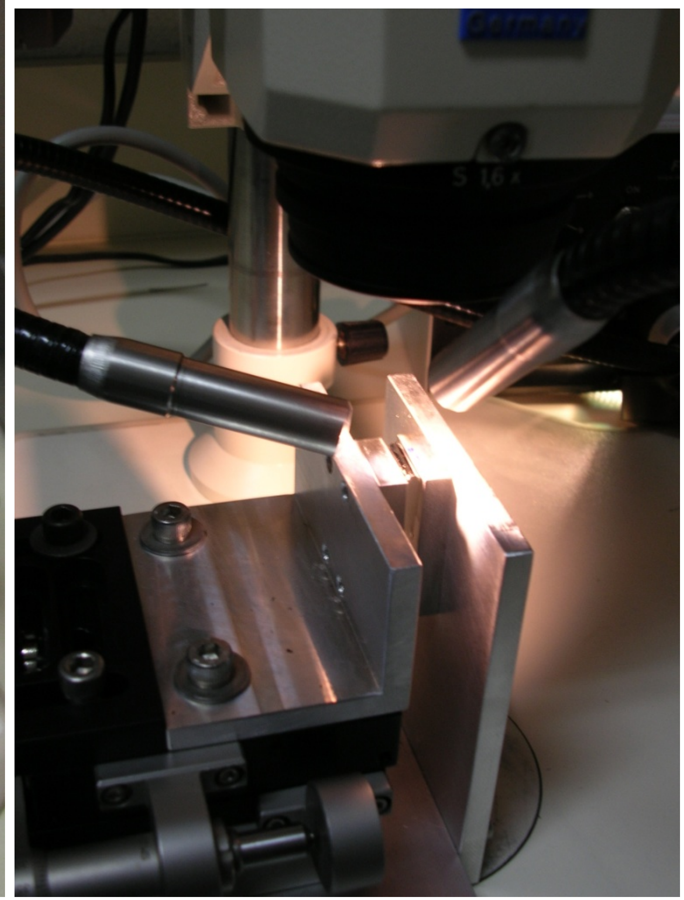

Effect of local favored structure on SB nucleation

- $Ni_{60}Nb_{40}$: fully amorphous phase **S=0.016 mm/sec**

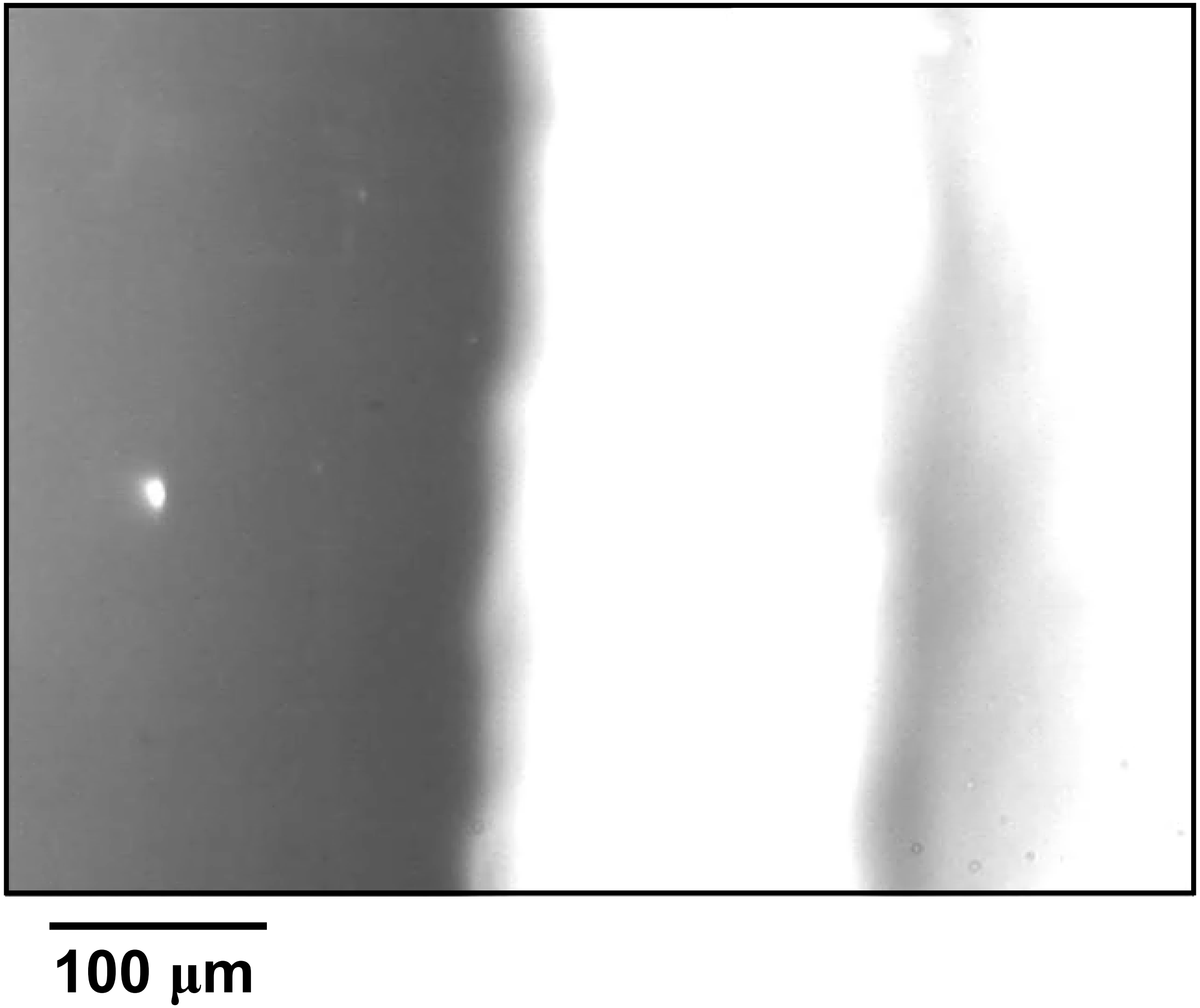

Effect of local favored structure on SB nucleation

- $Ni_{60}Nb_{20}Zr_{20}$: amorphous phase with local favored structure

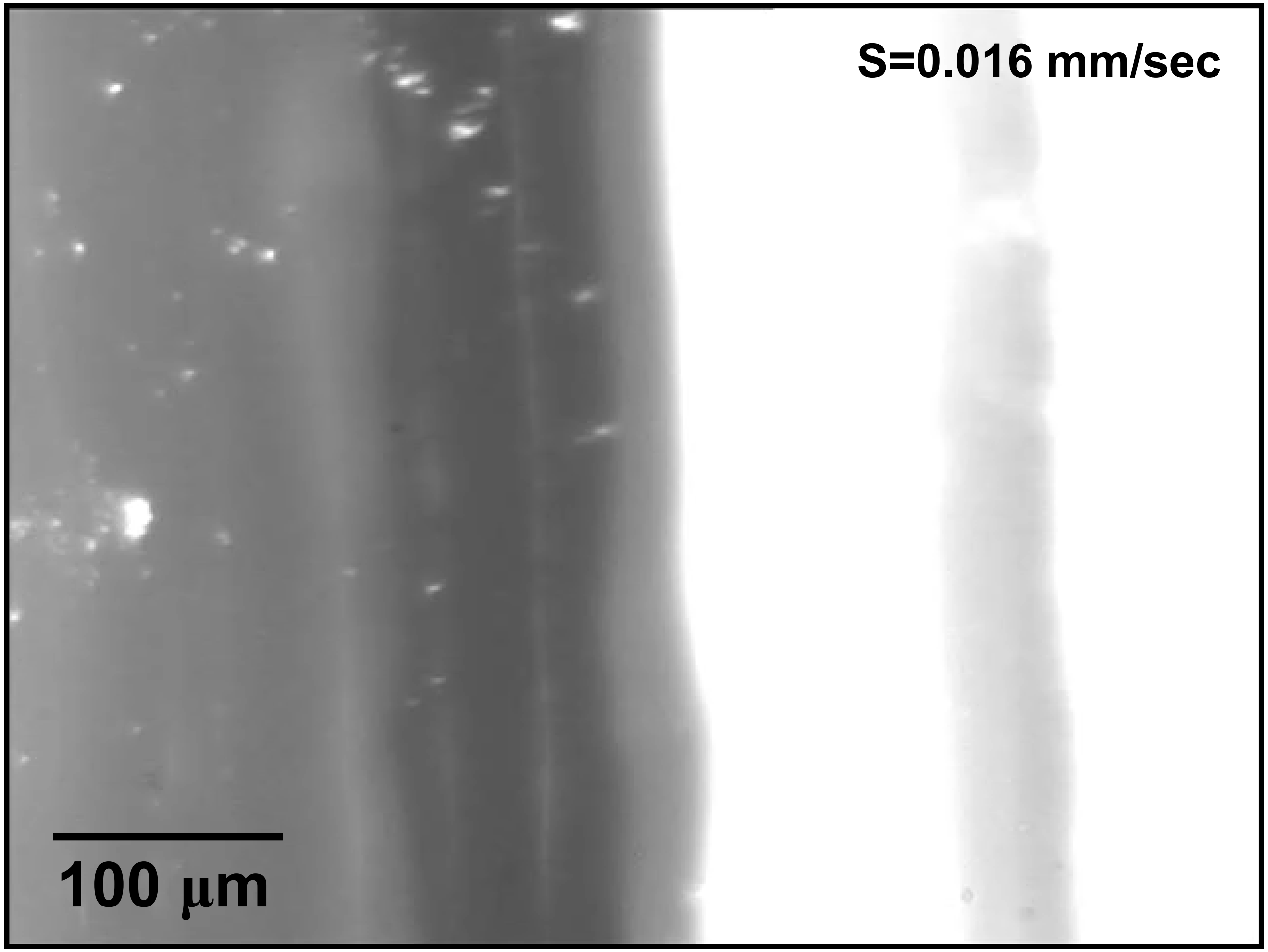

- **Increased nucleation sites of shear bands**

  ; evaluate the local heterogeneity in amorphous phase

Tailoring of structural inheterogeneity

- **Alloy design** + **Process control**

atomic scale inhomogeneity generation — Solidification under appropriate conditions

→ Enhanced plasticity in $Ni_{60}Nb_{32}Zr_8$, $Ni_{60}Nb_{30}Zr_{10}$ BMGs (σ_{max} : 3.2 GPa, ε_p : 2.5 %)

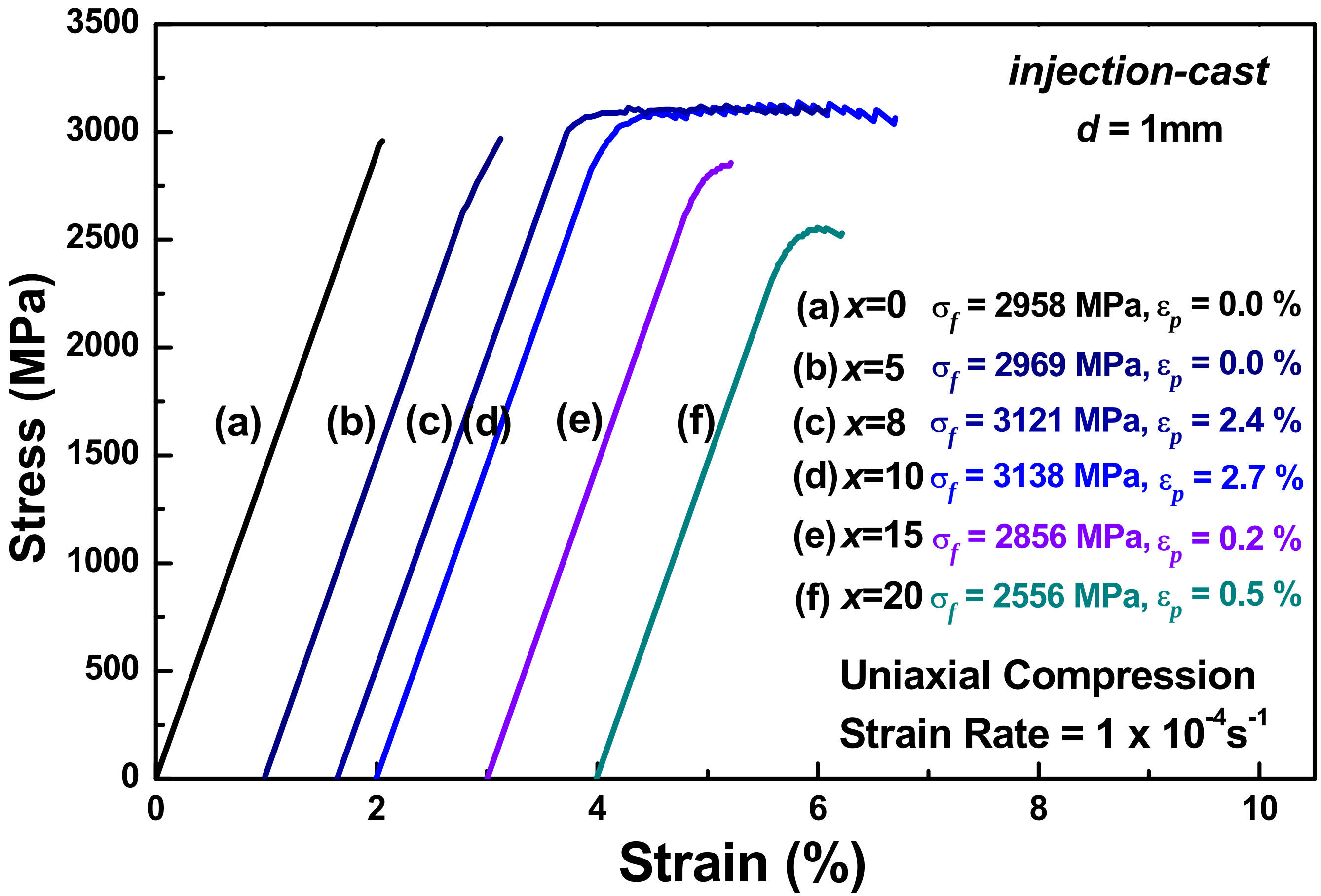

Bulk metallic glass matrix composites

(1) BMG matrix composites

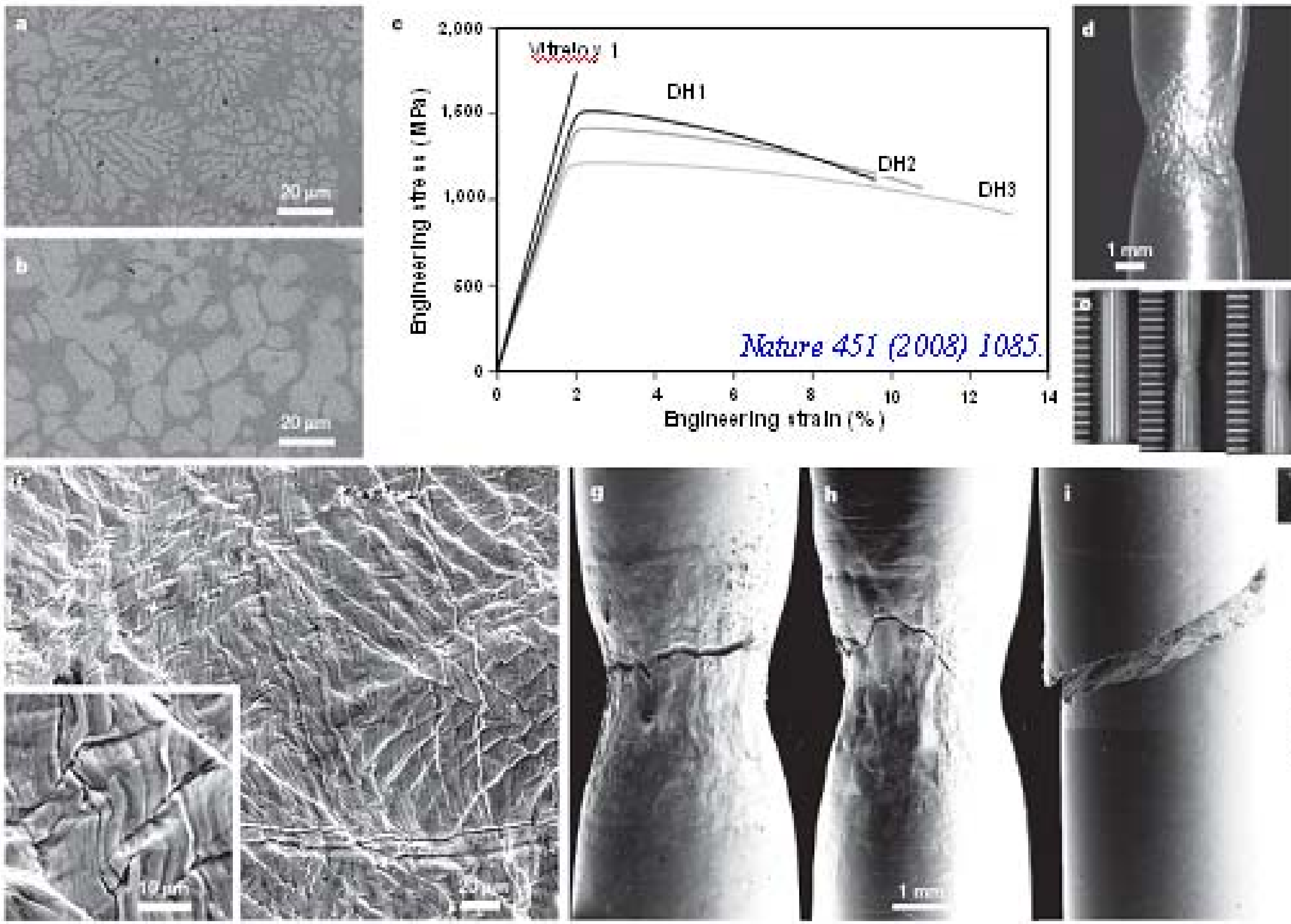

High fracture toughness: > 10 % plastic strain in tensile test

(2) Porous and foamed amorphous metals

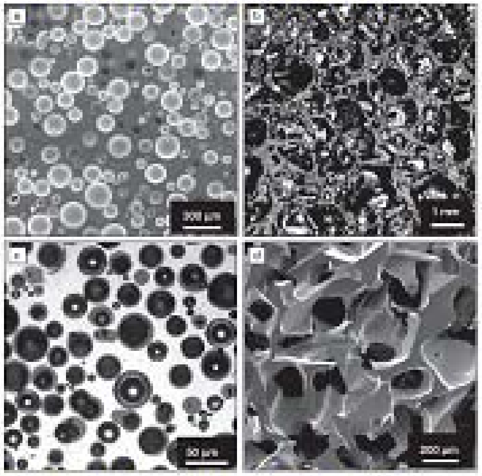

(3) Cold-rolled BMGs

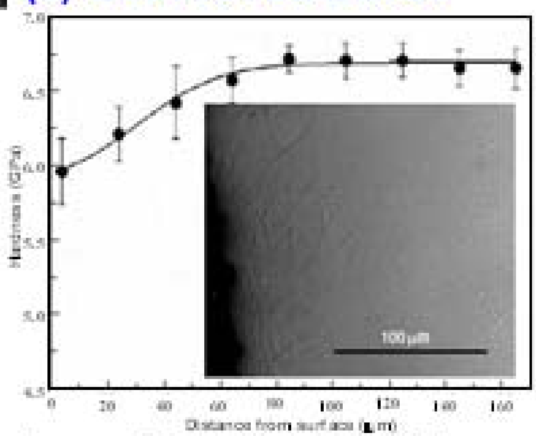

By control of residual stress

Nature Materials 5 (2006) 857.